Journal of Financial Stability 71 (2024) 101222

Contents lists available at ScienceDirect

Journal of Financial Stability

journal homepage: www.elsevier.com/locate/jfstabil

The topological structure of panel variance decomposition networks☆

Alessandro Celani [a], Paola Cerchiello [b], Paolo Pagnottoni [b,*]

[a] Department of Economics and Social Sciences, Università Politecnica delle Marche, Piazzale R. Martelli 8, Ancona, 60121, Ancona, Italy
[b] Department of Economics and Management, Via San Felice 5, Pavia, 27100, Pavia, Italy

ARTICLE INFO

JEL classification:
C40
E44
G01

Keywords:
Crisis
Global VAR
Network theory
Systemic risk
Variance decomposition

ABSTRACT

In this paper we provide a framework to study the network topology of generalized forecast error variance decomposition (GFEVD) derived from multi-country, multi-variable time series models. Our dynamic variance decomposition network is based on a Bayesian Global Vector Autoregressive (GVAR) model, a suitable macroeconometric method to consider simultaneous multi-level interdependencies across variables. We demonstrate the usefulness of our methodology to analyze the network structure of shock propagation in longitudinal time series and, in particular: (a) the shortest paths of contagion; (b) the clusters of shock transmission; (c) the role of nodes in the risk transmission channels. We illustrate our method through an empirical application to a set of 12 European countries' Industrial Production, Retail Trade and Economic Sentiment indices over the period 01/2000–11/2021.

1. Introduction

Globalization has considerably increased the interconnected nature of entities within the global economy and, thereby, their sensitivity to large shocks over the last few decades. Some of the benefits of globalization in terms of liberalization and development were contrasted by the emergence of the Global Financial Crisis, as a source of systemic risks posed by the financial globalization (Mishkin, 2011). Macroeconomic linkages feature different aspects of connectedness: trade linkages, financial linkages, and price changes (Dees et al., 2007). Hence, macroeconomic connectedness is a multi-dimensional concept, whose fragile equilibrium can be compromised by several risk sources. Extant literature has investigated the co-movements and support the notion of global business cycles, as drivers of co-movement in national business cycles — see Kose et al. (2003, 2008). While research on systemic risk linkages and financial connectedness has considerably advanced since then, a deep understanding of international macroeconomic linkages is still a basic open question, and the network structure of shock propagation across global economies is a ground to explore.

Large, unexpected exogenous shocks, such as the COVID-19 pandemic exert dramatic impacts on the financial and economic structure of countries (Delis et al., 2021; Pagnottoni et al., 2021; Iwanicz-Drozdowska et al., 2021; Spelta and Pagnottoni, 2021; Liu et al., 2021; Ahelegbey et al., 2022; Bitetto et al., 2021; Bartolucci et al., 2021). Recent groundwork in the financial context shows that the reaction of financial markets to exogenous shocks, such as climate related ones among the others, is increasingly harsher over recent years. Dafermos et al. (2018) shows how climate change has a significant effect on financial stability, as it causes a sudden drop in the level of liquidity injected to firms, as well as it reduces corporate bond prices, together with credit supply. Battiston et al. (2017) proposed a network-based climate value at risk to study risk transmission both system-wide and at institutional level, giving birth to a flourishing literature investigating the nexus between climate change and finance (Stolbova et al., 2018; Monasterolo et al., 2017; Battiston et al., 2019; Roncoroni et al., 2021; Battiston et al., 2021; Pagnottoni et al., 2022).

The modeling paradigm of current research in business cycle stems from methodologies which are not grounded on network theory – see Diebold and Yılmaz (2015) – although they present many complementary aspects to the systemic risk and to the complex network literature. Financial network econometric models include those developed by Billio et al. (2012), Diebold and Yilmaz (2009, 2012) and Diebold and Yılmaz (2014), in which individual entities can be represented as nodes in a financial network. While Billio et al. (2012)

☆ The peer-review for the present article was conducted outside of Elsevier's submission system. A record of this review was kept, and has been reviewed by the Publisher to ensure conformity with Elsevier's and the journal's standards for quality and ethics. Dates of submission and acceptance reflect the dates on which the final versions were uploaded to our submission system. The timeline for peer-review is available upon request. The Journal has now changed its policy to ensure that all peer review is conducted using Elsevier's Editorial Manager submission system.

* Corresponding author.
E-mail address: paolo.pagnottoni@unipv.it (P. Pagnottoni).

https://doi.org/10.1016/j.jfs.2024.101222
Received 7 February 2022; Received in revised form 14 July 2022; Accepted 6 November 2022
Available online 2 February 2024

develop causal networks based on the concept of Granger causality, Diebold and Yılmaz (2014) build generalized forecast error variance decomposition (GFEVD) on approximating Vector Autoregressive (VAR) models. Since then, the literature has started integrating time series econometrics approaches with network tools to assess systemic risk, particularly in financial market contexts — see e.g. Ahelegbey et al. (2016), Avdjiev et al. (2019) and Ahelegbey and Giudici (2022). More recently, Greenwood-Nimmo et al. (2021) developed a method to employ forecast error variance decomposition to evaluate the macroeconomic connectedness in any multi-country macroeconomic model with an approximate multi-country VAR representation. Therefore, such framework: (a) it is convenient in terms of interpretability; (b) it is able to take into account for contemporaneous impacts; (c) it can predictively measure system-wide and pairwise connectedness of time series networks.

Despite having the merit of being robust from a methodological perspective, state-of-the-art econometric models – based on forecast error variance decomposition – lack of a comprehensive framework in terms of their interpretation from a network analysis viewpoint. Diebold and Yılmaz (2014) and Greenwood-Nimmo et al. (2021) are key studies in this stream of research, as they relate network systemic risk measures based on forecast error variance decomposition, although without a strong link to network theory or topological analysis. The use of robust statistical methods to measure macroeconomic interconnectedness and systemic risk, combined with complex system methods – see, e.g. Battiston et al. (2016), Bardoscia et al. (2017) and Roukny et al. (2018) – is therefore a promising avenue for future research.

Against this background, we propose a network-based framework to investigate systemic risk, macroeconomic connectedness and lead–lag relationships from a set of multi-country and global macroeconometric models, i.e. Global Vector Autoregressive (GVAR) models. Our approach takes root from the forecast error variance decomposition spillover measures (Diebold and Yılmaz, 2014; Greenwood-Nimmo et al., 2021). We analyze the estimates of the econometric model by means of graph theory, studying clustering and hub-authority dynamics of the GVAR spillover network and its implications in terms of risk propagation mechanisms. This is done via the Minimum Spanning Tree (MST), the Louvain community detection and the Kleinberg algorithm, so to derive the backbone structure, communities and hub-authority dynamics of macroeconomic relationships. To this end, indices based on the decomposition of the variance–covariance matrix of the forecast error derived from the dynamic GVAR estimates are used, so to statistically and multidimensionally capture systemic risk in a predictive framework. We apply our methodology to study the spillover network of real economy and sentiment indicators of 12 European countries over the period 01/2000–11/2021 at the global, country and variable levels.

Similarly to our approach, Elhorst et al. (2018) bring together the spatial and GVAR classes of econometric models. Motivated by the study of spillovers, they define a measurable concept of spillover in this context based on impulse responses. Gross and Kok (2013) define a mixed-cross-section GVAR for forecasting and conducting systematic shock simulation. This eases the definition of spillover potential measures for within and across groups of sovereign and banks, also employing network centrality measures. In contrast, we examine the topological structure of GVAR spillover networks and its implications from a risk management perspective. In particular we study: (a) the shortest paths of contagion; (b) the clusters of shock transmission; (c) the role of nodes in the risk transmission channels. Additionally, we estimate a Bayesian GVAR, which encompasses also the maximum likelihood estimator as a special case, in order to cope with the possible presence of dominant units.

The contribution of this paper is twofold. From a methodology perspective, we extend the econometric GFEVD method illustrated by Greenwood-Nimmo et al. (2021) to a spillover network topology framework, which enables to study the complex dynamic network structure of the time series of forecast error variance shares, i.e. of spillovers. The combination of a robust global econometric model and the concepts of network theory results in a practical method for the development of a sound set of statistical network systemic risk indicators, which are based upon predictive directional measurement of spillovers. From an empirical viewpoint, our strategy allows to simultaneously examine: (a) the dynamic relationships of real economy and sentiment at a country level, identifying lead–lag relationships across EU member states over time; (b) the dynamic connectedness existing between real economy and sentiment variables.

The remainder of this paper is organized as follows. Section 2 introduces the proposed methodology. Section 3 describes the data used in our empirical study and conducts preliminary data analysis. Section 4 illustrates our empirical outcomes. Section 5 offers a final discussion.

2. Methodology

2.1. The global VAR model

Global VAR models are built on the premise that simple VAR models do well describe the linear dynamics of a system, although they suffer from the overparameterization problem, which makes their use impractical in high-dimensional contexts. Among the different approaches proposed in the literature to solve the curse of dimensionality, the GVAR proposed by Pesaran et al. (2004) and surveyed in Chudik and Pesaran (2016) provides a good framework to model a relative small set of variables shared by a fixed number of spatial units — which, in our case, represent countries.

The GVAR solves the dimensionality problem by decomposing the underlying large dimensional VAR into a smaller number of conditional models, which are linked together via cross sectional averages.

The first step consists of estimating small-scale country models enlarged by weakly exogenous and possibly global variables (VARX* model). Let $\mathbf{x}_{it}$ be a k_i dimensional vector of endogenous variables of country $i = 1, \dots, N$. We model each $\mathbf{x}_{it}$ as a VARX*(p_1, p_2):

$$\mathbf{x}_{it} = \boldsymbol{\alpha}_{i0} + \sum_{s=1}^{p_1} \boldsymbol{\Phi}_{is}\mathbf{x}_{i,t-s} + \sum_{r=0}^{p_2} \boldsymbol{\Lambda}_{ir}\mathbf{x}^*_{it-r} + \varepsilon_{it}, \tag{1}$$

where $\boldsymbol{\alpha}_{i0}$ is a vector of intercepts, $\boldsymbol{\Phi}_{is}$ $(s = 1, \dots, p)$ and $\boldsymbol{\Lambda}_{ir}$ $(r = 0, \dots, q)$ are, respectively, $k_i \times k_i$ and $k_i \times k_i *$ coefficient matrices of the lagged endogenous and the lagged weakly exogenous variables, and ε_{it} is an error term with covariance matrix Σ_i.

The country i weakly exogenous (or foreign) variables are calculated as a weighted average of the endogenous variables in all the other economies:

$$\mathbf{x}^*_{it} = \sum_{j=1}^{N} \omega_{ij} x_{jt} \tag{2}$$

with ω_{ij} representing a non-negative weight connecting country i and j. We assume that $\omega_{ii} = 0$ and $\sum_{j=1}^{N} \omega_{ij} = 1$. They reflect the relative magnitude of the interaction among economies and are usually approximated using data on bilateral trade flows. The underlying assumption of weak exogeneity of the foreign variables implies that most countries are small relative to the world economy.

By stacking the N country-specific models, we obtain the global one as an approximation of the large dimensional VAR :

$$\mathbf{G}_0\mathbf{x}_t = \boldsymbol{\alpha}_0 + \sum_{q=1}^{Q} \mathbf{G}_q\mathbf{x}_{t-q} + \varepsilon_t, \tag{3}$$

where $\boldsymbol{\alpha}_0$ is a $k \times 1$ vector of intercepts and $\mathbf{G}_q$ for $q = 0, \dots, Q$ are $k \times k$ coefficient matrices embodying contemporaneous and lagged dependence among countries, with $k = \sum_i k_i$ and $Q = \max(p_1, p_2)$. Finally, ε_t is the global error term with block diagonal covariance matrix Σ.

If the matrix $\mathbf{G}_0$ is invertible then, pre-multiplying (3) by $\mathbf{G}_0^{-1}$, we obtain the GVAR representation

$$\mathbf{x}_t = \mathbf{F}_0 + \sum_{q=1}^{Q} \mathbf{F}_q \mathbf{x}_{t-q} + \mathbf{G}_0^{-1}\varepsilon_t, \tag{4}$$

with $\mathbf{F}_0 = \mathbf{G}_0^{-1}\boldsymbol{\alpha}_0$ and $\mathbf{F}_q = \mathbf{G}_0^{-1}\mathbf{G}_q$ for $q = 1, \dots, Q$.

2.2. Bayesian estimation

The standard GVAR literature assumes that $\mathbf{x}_{it}^*$ are weakly exogenous, and therefore OLS is the most widely used estimation technique. However, such assumption can be violated when large economies are included in the analyzed sample. For this reason, it is preferable to perform maximum likelihood estimation of the GVAR (Elhorst et al., 2018).

In order to cope with the possible presence of dominant units, we refer to the maximum likelihood estimator as a special case of a Bayesian GVAR. Indeed, at the same time such an approach: (a) allows the researcher to specify her/his prior beliefs on the parameters of interest; (b) induces country-specific degrees of shrinkage on the parameters, which improves forecast in a significant way.

The prior implementation is facilitated by rewriting each country model compactly as:

$$\mathbf{x}_{it} = \boldsymbol{\Pi}_i' \mathbf{z}_{it-1} + \varepsilon_{it}, \tag{5}$$

where $\mathbf{z}_{it-1} = [1, \mathbf{x}_{it-1}', \dots, \mathbf{x}_{it-p_1}', \mathbf{x}_{it}^{*\prime}, \dots, \mathbf{x}_{it-p_2}^{*\prime}]'$ is the K_i dimensional vector of regressors, with $K_i = 1 + k_i p_1 + k_i^*(p_2 + 1)$, and $\boldsymbol{\Pi}_i' = [\boldsymbol{\alpha}_{i0}, \boldsymbol{\Phi}_{i1}, \dots, \boldsymbol{\Phi}_{ip_1}, \boldsymbol{\Lambda}_{i0}, \dots, \boldsymbol{\Lambda}_{ip_2}]'$ is the associated matrix of stacked coefficients. The model specification is completed by assuming that $\boldsymbol{\varepsilon}_{it}$ are normally distributed:

$$\boldsymbol{\varepsilon}_{it} \sim \mathcal{N}(0, \Sigma_i). \tag{6}$$

In order to derive a compact form, Eq. (5) can be rewritten as a multivariate linear regression:

$$\mathbf{X}_i = \mathbf{Z}_i \boldsymbol{\Pi}_i + \boldsymbol{\varepsilon}_i, \tag{7}$$

where $\mathbf{X}_i$ is a $T \times k_i$ matrix of endogenous variables, $\mathbf{Z}_i$ is a $T \times K_i$ matrix of stacked explanatory variables and $\boldsymbol{\varepsilon}_i$ is a matrix of errors.

Following Cuaresma et al. (2016), we employ the Normal-Inverse Wishart prior, which belongs to the class of natural conjugate priors. Let $\boldsymbol{\Psi}_i = \text{vec}(\boldsymbol{\Pi}_i)$ denote the $v_i = K_i k_i$ dimensional coefficient vector. The prior setting reads as:

$$\boldsymbol{\Psi}_i | \Sigma_i \sim \mathcal{N}(\underline{\boldsymbol{\Psi}}_i, \Sigma_i \otimes \underline{\boldsymbol{V}}_i), \tag{8}$$

$$\Sigma_i \sim \mathcal{IW}(\underline{S}_i, v_i). \tag{9}$$

Following the literature on Bayesian VARs (Litterman, 1986; Sims and Zha, 1998), we assume that the variables in the system follow simple random walks. This results in imposing $\underline{\Psi}_i = 1$ for the entries concerning the first own lag of each endogenous variable, $\underline{\Psi}_i = 0$ otherwise. Regarding the elicitation of $\mathbf{V}_{i0}$, we specify a Minnesota prior. In particular, for the parameters in $\boldsymbol{\Psi}_i$ corresponding to lag r of variable g, it is given by:

$$\underline{\boldsymbol{V}}_{i,gr} = \begin{cases} \frac{\alpha_1}{r^k \sigma_{ig}} & \text{for the } r-th \text{ lag of variable } g \\ \frac{\alpha_2}{(1+r)^k \sigma_{ig}^*} & \text{for the } r-th \text{ lag of variable } g \text{ if weakly exogenous} \\ \alpha_3 & \text{for the constant term} \end{cases} \tag{10}$$

where α_1 and α_2 are hyperparameters controlling the tightness of the prior on the endogenous and weakly exogenous parts respectively, σ_{ig} and σ_{ig}^* are standard deviations obtained by estimating univariate regressions on the gth endogenous variable and gth exogenous one, α_3 controls the tightness of the prior on the constant term. For a detailed explanation of the prior setup see Cuaresma et al. (2016).

Given the high cross-sectional dimension handled by the GVAR, it is not necessary to employ a long lag length as in a standard VAR (Burriel and Galesi, 2018). Hence we set $p_1 = p_2 = 1$ for the country models. Regarding the hyperparameters, we remain quite uninformative through a relatively flat prior, hence we set $\alpha_1 = \alpha_2 = \alpha_3 = 100$. Such configuration allows to produce results approaching the ML ones.

2.3. Forecast error variance decomposition in global VARs

Our approach stems from the econometric connectedness measures developed by Diebold and Yilmaz (2009, 2012) and Diebold and Yılmaz (2014), which generally assume a stationary approximating time series VAR model, and that we apply to the GVAR modeling framework. Diebold and Yılmaz (2014) build generalized forecast error variance decomposition (GFEVD) on approximating Vector Autoregressive (VAR) models. The idea behind this approach is that the more a variable is important in forecasting the future dynamics of another, the more a shock in the former impacts the time series trajectory of the latter.

More recently, in line with our methodology, Greenwood-Nimmo et al. (2021) develop a method to employ forecast error variance decompositions to evaluate the macroeconomic connectedness in any multi-country macroeconomic model with an approximate VAR representation. They build their research on Diebold and Yılmaz (2014) and, particularly, on the shortcoming of not correctly dealing with high-dimensional cross-section data series and with an increasing number of variables m. This framework presents several advantages. In particular, it is convenient in terms of interpretability, it is able to take into account for contemporaneous impacts and it can measure predictively measure system-wide and pairwise connectedness in terms of direction and magnitude of network links.

The methodology by Greenwood-Nimmo et al. (2021) overcomes both the curse of dimensionality, which generally calls for a low number of variables m in empirical applications, and for the need of accommodating intermediate levels of aggregation in the modeling strategies, in a multilevel perspective. They propose a simple approach to overcome both issues based on re-normalization and block aggregation of the connectedness matrix. The exposition of the block aggregation routine exploits the fact that GFEVDs are invariant to the ordering of variables in the VAR model. We refer the reader to Appendix A.1 for further methodological details on the Global GFEVD techniques to derive the econometric spillover measures.

Within this framework, the total *from*, *to* and *net* connectedness of the kth group are respectively defined as follows:

$$\mathcal{F}_{k\leftarrow\bullet}^{(n)} = \sum_{\ell=1,\ell\neq k}^{b} \mathcal{F}_{k\leftarrow\ell}^{(n)}, \tag{11}$$

$$\mathcal{T}_{\bullet\leftarrow k}^{(n)} = \sum_{\ell=1,\ell\neq k}^{b} \mathcal{T}_{\ell\leftarrow k}^{(n)}, \tag{12}$$

$$\mathcal{N}_{\bullet\leftarrow k}^{(n)} = \mathcal{T}_{\bullet\leftarrow k}^{(n)} - \mathcal{F}_{k\leftarrow\bullet}^{(h)}, \tag{13}$$

where $\mathcal{F}_{k\leftarrow\bullet}^{(\text{h})}$ measures the total spillover from all other groups to group k, the total *from* contribution affecting group k.

$\mathcal{T}_{\bullet\leftarrow k^{(1)}}$ measures the total spillover to all other groups from group k, the total *to* contribution arising from group k.

$\mathcal{N}_{\bullet\leftarrow k}^{(n)}$ is the net connectedness of group k. The subscript $i \leftarrow \bullet$ indicates that the directional effect is from all other variables to variable i.

It is possible to derive in a similar way the aggregate heatwave and spillover indices, expressed in terms of the b groups, as:

$$\mathcal{H}^{(n)} = \sum_{k=1}^{D} \mathcal{W}_{k\leftrightarrow k}^{(h)}, \tag{14}$$

$$\mathcal{S}^{(n)} = \sum_{k=1}^{b} \mathcal{F}_{k\leftarrow\bullet}^{(n)} \equiv \sum_{k=1}^{b} \mathcal{T}_{\bullet\leftarrow k}^{(n)}, \tag{15}$$

where $\mathcal{H}^{(n)} + \mathcal{S}^{(h)} = 1$ and $\sum_{k=1}^{D} \mathcal{N}_{\bullet\leftarrow k}^{(h)} = 0$, $\forall h$ by construction. Differently from the variable-level heatwave and spillover measures, in $\mathcal{H}^{(h)}$ and $\mathcal{S}^{(h)}$ measure the heatwave and spillover effects in a consistent way with respect to an aggregation routine.

From above, one can derive also two indices which are key to evaluate interconnectedness among entities and small group of entities, such as geopolitical units and financial market sectors. They express either how dependent is the kth group on external conditions or to which degree does the kth group influences the kth group or it is influenced by the system as a whole. The first measure is the dependence index:

$$\mathcal{O}_k^{(h)} = \frac{\mathcal{F}_{k\leftarrow\bullet}^{(h)}}{\mathcal{W}_{k\leftarrow k}^{(h)} + \mathcal{F}_{k\leftarrow\bullet}^{(h)}}. \tag{16}$$

The index measures the relative importance of external shocks for the kth group. In particular, as $\mathcal{O}_k^{(h)} \to 1$, the network structure of group k is dominated by external shocks, while group k is unaffected by external shocks if $\mathcal{O}_k^{(h)} \to 0$. Similarly, the influence index can be derived as:

$$\mathcal{I}_k^{(h)} = \frac{\mathcal{N}_{\bullet\leftarrow k}^{(h)}}{\mathcal{T}_{\bullet\leftarrow k}^{(h)} + \mathcal{F}_{k\leftarrow\bullet}^{(h)}}, \tag{17}$$

where $-1 \leq \mathcal{I}_k^{(h)} \leq 1$. For any horizon h, the kth group is a net shock recipient if $-1 \leq \mathcal{I}_k^{(h)} < 0$, a net shock transmitter if $0 < \mathcal{I}_k^{(h)} \leq 1$, and neither of the two if $\mathcal{I}_k^{(h)} = 0$. Hence, the influence index expresses the extent to which the kth group influences or is influenced by conditions in the system. When studying connectedness among countries, the coordinate pair $\left(\mathcal{O}_k^{(h)}, \mathcal{I}_k^{(h)}\right)$ in dependence-influence space can give a good representation of country (or variable) k and its role in the global network system. While small open economies would tend to be located close to the coordinates $(1, -1)$, a dominant economy would lay in the proximity of $(0, 1)$.

We remark that the GFEVD has the inherent characteristic of not reflecting the impact of structural shocks, but only composite ones, an approach which suffers from the contemporaneous correlation across equation innovations. The GFEVD as opposed to the orthogonal FEVD is however more readily determinable without the need of incurring in identification schemes which could result into questionable choices.

2.4. Network theory and forecast error variance decompositions

In general, a variety of network analysis approaches, which study the structure and interactions of weighted directed network, can be applied to any econometric connectedness matrix derived from GFEVD which assumes the form:

$$\underset{(m\times m)}{\mathbb{C}^{(h)}} = \begin{bmatrix} \phi_{1\leftarrow 1}^{(h)} & \phi_{1\leftarrow 2}^{(h)} & \cdots & \phi_{1\leftarrow m}^{(h)} \\ \phi_{2\leftarrow 1}^{(h)} & \phi_{2\leftarrow 2}^{(h)} & \cdots & \phi_{2\leftarrow m}^{(h)} \\ \vdots & \vdots & \ddots & \vdots \\ \phi_{m\leftarrow 1}^{(h)} & \phi_{m\leftarrow 2}^{(h)} & \cdots & \phi_{m\leftarrow m}^{(h)} \end{bmatrix}, \tag{18}$$

where $\phi_{i\leftarrow j}^{(h)}$ represents the contribution of variable j to the h -steps-ahead forecast error variance of variable i. Similarly, $\phi_{i\leftarrow i}^{(h)}$ denotes the contribution of variable i to its own h-steps-ahead forecast error variance (see Appendix A for further details on the connectedness matrix). Another important issue is the dimensionality of the Global GFEVD directional spillover network matrix. Indeed, given the ability of the GVAR to handle large number of variables, it allows to derive high-dimensional GFEVD matrices. However, these matrices are fully connected. This calls for the implementation of tools borrowed from network theory and topological analysis to study backbone structures, centrality measures, hub-authority relationships and many more network analysis approaches on econometric connectedness measures – see also Pagnottoni (2023) and Pagnottoni and Spelta (2023).

In this context, we propose to merge two very consolidated approaches – i.e. financial econometrics and network theory – to investigate dominant links existing in the matrix of time series GFEVD from two different perspectives, and, at the same time, in a complementary way. In particular, we investigate the network topology of the risk spillover matrix coming from the Global VAR generalized forecast error variance decomposition. In other words, we employ the MST, the Louvain community detection and the Kleinberg centrality measure so to study the backbone structure and the hub-authority dynamics of macroeconomic relationships, on indices based on the decomposition of the variance–covariance matrix of the forecast error derived from the dynamic GVAR estimates.

The combination of the two methodologies presents two main practical advantages. First, we are able to statistically capture systemic risk in a multi-country and multi-variate way, either at the aggregate or individual level, and within a predictive framework. Second, we benefit from enhanced explainability of results and insights derived from the network analysis of econometric measures of systemic risk in the two specific dimensions of the longitudinal time series.

2.4.1. Minimum spanning tree

In order to simplify the relationships given by the GFEVD matrix, we apply the Minimum Spanning Tree (MST) representation. This is a widely employed technique in finance — see, for instance, Micciché et al. (2003) and Musciotto et al. (2018). The Kruskal's algorithm, which delivers the minimum spanning tree from a given adjacency matrix, is able to reduce the number of links among the nodes by drawing a link for each node to its closest neighbor. In this way, we achieve dimensionality reduction of the GFEVD spillover matrices obtained from the Global VAR estimation, and we are able to determine the backbone structure of both countries and variables.

The methodological premise of the Minimum Spanning Tree (MST) is the existence of a given weighted graph $G = [V, E]$, with $v \in V$ vertices and $e \in E$ weighted edges. Without loss of generality, the weights can be thought as the cost to reach v_j from v_i. We are interested in finding a subgraph $\tilde{G}$ of G such that $V(G) = V(\tilde{G})$ (i.e. they span the same nodes) but with the minimum possible aggregate cost, thought as the sum of all the graph weights.

Let us define $ST(G)$ as the spanning tree set generated by the graph G, i.e. the set of all trees that spans all the nodes of G. $\hat{G} \in ST(G)$ is called a minimum weight spanning tree if the sum of the weights of the edges of $\hat{G}$ does not exceed the sum for any other spanning tree of G (i.e. the one that minimizes the sum of weights of the set $ST(G)$), see Harris et al. (2008).

There are a variety of algorithms for exploiting minimum weight spanning trees. The most widespread and employed is the Kruskal's algorithm, which can be summarized as follows. Given a connected, weighted graph G:

1. Find an edge of minimum weight and mark it.
2. Among all of the unmarked edges that do not form a cycle with any of the marked edges, choose an edge of minimum weight and mark it.
3. If the set of marked edges forms a spanning tree of G, then stop. If not, repeat step 2.

2.4.2. Louvain clustering for community detection

An important feature of complex networks is its community structure, which refers to the presence of groups of nodes. Each group contains a set of nodes; within each group the density of edges is higher than that among the groups. Community detection algorithms might reveal the hidden relations among the nodes in a network. The core of the Louvain method (Blondel et al., 2008) is to find a partition of the vertex set that maximizes the modularity of the considered graph. This function provides a way to value the existence of an edge between two vertices of an undirected network by comparing it with the probability of having such an edge in a random model.

Modularity is a measure of the topology of networks, representing the degree to which a network is fragmented into communities. A high modularity corresponds to a network with dense links within community nodes, but sparse links between the nodes belonging to different communities. This is of relevance when analyzing financial and economic spillover networks, since it reveals information on the communities involved in the risk propagation mechanism, as well as on shock-resilient entities. Formally, the modularity Q of a partition C of an undirected graph $G = (V, E)$ is defined as follows :

$$Q = \frac{1}{2m}\sum_{i,j}\left[A_{ij} - \frac{d_i d_j}{2m}\right]\delta\left(c_i, c_j\right) \tag{19}$$

where m stands for the number of edges of G, A_{ij} represents the weight of the edge between i and j, d_i is the degree of vertex i (i.e. the number of neighbors of i), c_i is the community the vertex i belongs to and δ is the so called Kronecker delta function, defined as $\delta(u, v) = 1$ if $u = v$, 0 otherwise.

Louvain's algorithm relies on a greedy procedure. First, each node is assigned to its own community. Then the algorithm tries to increase the value of modularity by moving nodes into the community of each neighbor. In other words, the algorithm computes the gain of modularity obtained by adding vertex i to community C as follows:

$$\begin{aligned}\Delta_Q &= \left[\frac{\sum_{in}+d_i^C}{2m} - \left(\frac{\sum_{tot}+d_i}{2m}\right)^2\right] - \left[\frac{\sum_{in}}{2m} - \left(\frac{\sum_{tot}}{2m}\right)^2 - \left(\frac{d_i}{2m}\right)^2\right] \\ &= \frac{d_i^C}{2m} - \frac{\sum_{tot}\cdot d_i}{2m^2}\end{aligned} \tag{20}$$

where d_i^C denotes the degree of node i in community C, $\sum_{in}$ the number of edges contained in community C and $\sum_{\text{tot}}$ the total number of edges incident to community C.

Once this value is derived for all communities i is connected to, i is placed where the value of the modularity is maximized. If no increase is possible, i remains in its original community. This process is applied repeatedly and sequentially to all nodes until there are no moves that improve the value of modularity. We remark that the main difference between the Louvain and K-means methodologies is that the former is nonparametric, and requires no a priori assumptions on the graph. Moreover, K-means and most of the clustering techniques act on data points embedded in a space, while Louvain on data points linked by an underlying graph.

2.4.3. Hubs and authorities

In this paper we employ a well-known centrality measure in order to explore the centrality and, thereby, hubs, authorities and systemically important nodes in the Global VAR macroeconomic system GFEVD framework. Network theory includes several centrality measures such as the degree centrality, counting how many neighbors a node has, as well centrality measures based on properties of graphs. Among centrality measures we remark Katz's centrality – see Katz (1953) – PageRank – (Brin and Page, 1998) –, hub and authority centralities, and the eigenvector centrality - (Bonacich, 2007).

In our context, we aim at investigating hub-authority network centralities of country and variable systems, which can be derived through the Kleinberg centrality measure. According to such centrality measure, a node is important if it has many incoming links from other important nodes. In general, nodes with no incoming links cumulate, in the best case, only to a minimum amount of centrality. However, it can also be argued that a node is important, even if not pointed by many others, if it links to a set of important vertices. Hence, there are two kinds of central nodes: *authorities*, that contain reliable information, and *hubs*, that suggest (point) where to find reliable information. The first ones are pointed by many good hubs nodes, and, conversely, the second ones point to many good authorities vertices.

For each node of a graph, we use $au(x)$ to denote its authority score and $hu(x)$ its hub score. We start by setting $au(x) = hu(x) = 1$ for all nodes. The core of the algorithm is an iterated update of the hub and authority scores of all nodes given by (21), which capture the intuitive notions that good hubs point to good authorities and that good authorities are pointed to by good hubs:

$$\begin{aligned}hu(x) &= \sum_{k\in Pa(x)} au(k), \\ au(x) &= \sum_{k\in Ch(x)} hu(k),\end{aligned} \tag{21}$$

where $Pa(x)$ is the set of parents of node x and $Ch(x)$ is the set of children of x. The first line of (21) sets the hub score of a node v to the sum of the authority scores of the nodes it links to. In other words, if v links to nodes with high authority scores, its hub score increases. The second line plays the reverse role; if node v is linked to by good hubs, its authority score increases. Let us shift (21) into matrix form. Let Au and Hu denote the vectors of all hub and all authority scores respectively. Let D denote the adjacency matrix of this graph: it is a square matrix with entry $D_{ij} = 1$ if there a edge from node i to j, and 0 otherwise. Then, we may write (21) as:

$$\begin{aligned}Hu &= D'Au, \\ Au &= DHu.\end{aligned} \tag{22}$$

Substituting Au (Hu) in the second (first) equation with the right hand of the first (second) one we can rewrite (22) as:

$$\begin{aligned}Hu &= DD'Hu \\ Au &= D'DAu.\end{aligned} \tag{23}$$

If we introduce the (unknown) eigenvalue, the first line of (23) becomes the equation for the eigenvectors of DD', and the second becomes the equation for the eigenvectors of $D'D$:

$$\begin{aligned}Hu &= \frac{1}{\lambda_a}DD'Hu \\ Au &= \frac{1}{\lambda_h}D'DAu\end{aligned} \tag{24}$$

where λ_a and λ_h are, respectively, the eigenvalues of DD' and $D'D$. The iterative process introduced in (21) is equivalent to the problem of solving the characteristic equation of matrices by finding the principal eigenvectors (and eigenvalue) of DD' and $D'D$. The resulting computation thus takes the following form, once the weighted graph is available:

1. Compute $D'D$ and $D'D$
2. Compute the principal eigenvectors of $D'D$ and DD' to form the vector of hub scores Hu and authority scores Au.
3. Rank the vectors found to check which subset of nodes in the graph have the highest hub and authority values.

3. Data

Our empirical exercise encompasses real economy and economic sentiment indicators, as measured by the Economic Sentiment indices survey data provided by EUROSTAT. We analyze a selected set of real economy and survey sentiment data variables for 12 countries in Europe, namely: Austria, Belgium, Denmark, France, Germany, Ireland, Italy, Netherlands, Poland, Spain, Sweden and United Kingdom. Such choice is due to data availability and quality constraints thus, the analyzed 12 countries, assure full and complete timeseries. Nevertheless, these 12 countries cover more than 90% of the European Union's GDP.[1] As Great Britain left EU in January 2020, we rely on previous years statistics. In particular, we analyze the time series of Industrial Production, Retail Trade and Economic Sentiment over the period 01/2000–11/2021. We select four crucial periods for the analysis of critical transitions in the real economy and economic sentiment:

[1] Source: EUROSTAT Database.

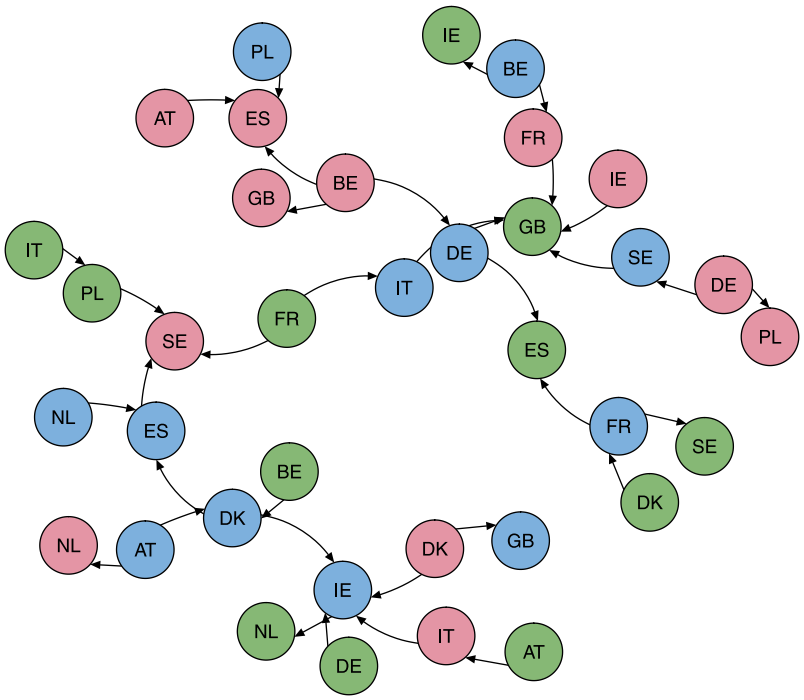

Fig. 1. Global forecast error variance Minimum Spanning Tree (MST). The figure shows a graphical representation of the MST calculated on the generalized forecast error variance decomposition (GFEVD) relative to the whole sample period. Network nodes represent system variables, whereas edges represent the directional contribution of each variable to the forecast error variance decomposition of the others. Colors stand for Industrial Production (red), Retail Trade (green) and Economic Sentiment (blue). Self-loops are omitted. (For interpretation of the references to color in this figure legend, the reader is referred to the web version of this article.)

- Phase 1: The pre-crisis period (01/2006–08/2008);
- Phase 2: The Global Financial and European Sovereign Debt crises period (09/2008–12/2012);
- Phase 3: the post-crisis period (01/2013–02/2020);
- Phase 4: The COVID-19 pandemic period (03/2020–11/2021).

Before the modeling exercise, we test the assumption that the country-specific foreign variables are weakly exogenous, i.e. we test for the presence of dominant units. This ensures the consistent estimation of the number of cointegrating relationships and the cointegrating vector for each country model in a separate way. We refer the reader to Chudik and Pesaran (2013), Konstantakis et al. (2015) and Pesaran and Yang (2020) for thorough discussions on dominant units. Details and results on the weak exogeneity test are contained in Appendix B.2.

In summary, the weak exogeneity assumptions are violated in 3 cases out of 21. The first one pertains Industrial Production of UK, which is consistent with Dees et al. (2007), who found a rejection in the UK country model. The second and third ones are related to Retail Trade of Austria and Sweden. Given these premises, we have opted for a more consistent estimation procedure through the Bayesian GVAR outlined in the methodological section.

4. Empirical results

4.1. Global analysis

Our global analysis examines the interaction between real economy and sentiment both at the country and variable levels. In particular, we first show the degree of cointegrating relationships existing among our data variables. After that, we show the network structure of the GFEVD of the three variables of interest – i.e. Industrial Production, Retail Trade and Sentiment indices – across the 12 European countries under consideration.

Fig. 1 shows a graphical representation of the Minimum Spanning Tree calculated on the generalized forecast error variance decomposition (GFEVD) relative to the whole sample period. Network nodes represent system variables, whereas edges represent the directional contribution of each variable to the forecast error variance decomposition of the others. The MST paths retained are represented by edges with larger weights of GFEVD transmitted to the other nodes, highlighting the backbone structure of the GFEVD spillover network. We notice a central role of the French Retail Trade index, which acts as a bridge and shock transmitter towards two consistent sub-graphs, particularly by means of its link with the Industrial Production index of Estonia and with the Economic Sentiment of Italy. The two sub-graphs, divided in this way, differ significantly in composition. The first one is mainly composed by Industrial Production variables, with Austria, Spain, United Kingdom and Belgium being – directly or indirectly – linked. The second sub-graph is mainly composed by Economic Sentiment and Retail Trade indices. In this case, sentiment variables of Netherlands, Spain, Denmark, Austria and Ireland influence each other in the context of the network backbone structure.

Fig. 2 shows the clustered GFEVD network structure of real economy and economic sentiment variables over the full sample period, where clusters are obtained through the Louvain community detection algorithm. Results highlight the emergence of four clusters: two of them are clearly denser than the other two. The largest cluster (pink) mainly consists of Retail Trade variables, whereas the second largest (blue) shows a prevalence of Economic Sentiment and Industrial Production variables, with many country-specific connections. Interestingly, the GFEVD network clusters show the emergence of two relatively isolated, but still communicating vessels. The first one (purple) is composed by the Industrial Production of Poland, the Retail Trade of Italy and Sweden, along with the Economic Sentiment of Sweden and Belgium. In the second group (green), we find the Industrial Production indices of Italy and Belgium and the Economic Sentiment of Italy and Spain. The strongest link is that between the Economic Sentiment and the Industrial Production of the Italy, which has strongly co-moved over the last two decades, and acts as a main information bridge across clusters.

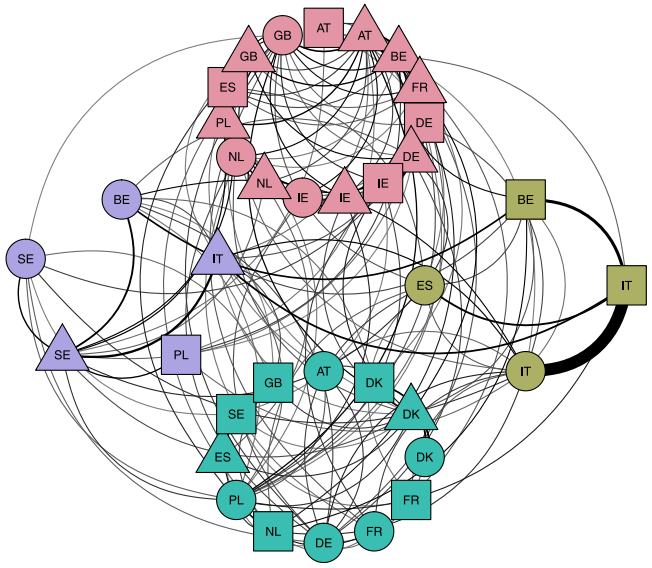

Fig. 2. Global forecast error variance clustering. The figure shows the clustered generalized forecast error variance decomposition (GFEVD) network structure of real economy and economic sentiment variables, where groups are classified according to the Louvain clustering algorithm. Squares: Industrial Production; triangles: Retail Trade; circles: Economic Sentiment.

4.2. Variable analysis

The aim of the variable analysis is to investigate the informationally dominant variables, in terms of GFEVD transmitted to others, in the network of variables (Industrial Production, Retail and Sentiment indices) over time. The analysis at a variable level aggregates country GFEVD and derives overall predictive spillovers from one variable to another. Based on this, we derive the aggregate dependence and influence indices of the sentiment and real economic variables, so to measure the role played in the system at an aggregate level.

In this regard, Fig. 3 shows the scatter plot obtained by generating a cartesian plane with the influence index on the x axis and the dependence index on the y axis, as defined in Section 2. Both the indices are calculated starting from the aggregation of the three variables of interest (Industrial Production, Retail and Sentiment indices) at the country level of the GFEVDs.

From the temporal dynamics along the 4 considered periods, we observe that the three first phases are quite similar, the main difference lies in the position of the Retail Trade index which swings between negative and positive values with regards to the influence index. That said, the most interesting pattern appears, once again, when considering the last period of crisis: the ranking of the indices is inverted and in particular the sentiment index presents a negative value for the influence, meaning that it is more influenced than before. This might be linked to the fact that, being COVID-19 a large and, most of all, unexpected exogenous shock to the network of real economic and sentiment interrelationships, it does cause a reversal of trend between sentiment and the real economy. While macroeconomic expectations have mostly tended to anticipate real macroeconomic dynamics in view of current situations, such a strong unexpected shock has swapped the relationship and led the real economic conditions to dominate the dynamics of sentiment.

4.3. Country analysis

In the country analysis, we investigate country-level connectedness in terms of time series dynamics of real economic and sentiment variables. In particular, we first show the dynamic Aggregate Heatwave and Spillover index, so to give an idea of the magnitude of the interaction within- and cross-country GFEVD. Then, we examine the dependence and influence of each of the European countries in terms of transmitted/received economic and sentiment GFEVD spillovers. Finally, we study the hub-authority relationships across countries in terms of their contribution to the others with regards to the forecast error variance.

Table 1
Country-level network hubs. The table reports countries ranked in decreasing order along with their normalized "Hubs" values (in brackets) calculated on the directed network of country block GFEVDs divided into the four sub-samples under consideration.

	1st	2nd	3rd	4th	5th
Phase 1	Net (12.860)	Bel (11.333)	UK (10.173)	Pol (10.033)	Ire (8.385)
Phase 2	Net (24.101)	UK (12.968)	Pol (8.958)	Ger (8.024)	Pol (7.862)
Phase 3	Ger (12.957)	Spa (10.826)	Pol (10.594)	Net (10.579)	Ita (9.697)
Phase 4	Ger (17.768)	UK (14.555)	Pol (11.065)	Fra (9.427)	Net (9.426)

Fig. 4 shows the Aggregate Heatwave and the Overall Spillover index based on the dynamic GFEVDs. The beginning of the Global Financial Crisis (September 2008) and the COVID-19 outbreak (February 2020) are marked in red. The two crisis periods emerge clearly from the curves dynamics with huge drops (hypes) followed by recovery periods. In particular, evidence shows that during both the Global Financial Crisis and the COVID-19 pandemic, the interconnectedness (Aggregate Heatwave) within country variables decreases sharply, likely due to large misalignment in the real economy and sentiment time series dynamics. Similarly, the between-country interconnectedness (Spillover index) starkly rises because of increased connection between countries' real economies and sentiment. Interestingly, the COVID-19 impact seems to be more persistent in time than that exerted by the Global Financial Crisis in terms of spillover magnitude.

Fig. 5 shows the directed weighted GFEVD spillover network obtained from the country aggregation of the whole sample GFEVD. Nodes represent countries, whereas links represent the magnitude of pairwise directed forecast error variance transmitted to others. The central role is played by Germany which shows strong directed links with eight countries. Some other countries such as Poland, Ireland and Denmark seem to be overall more peripheral in the spillover network, as well as mostly GFEVD receivers than transmitters. Such results need to be, however, analyzed from a dynamic perspective in order to capture the evolution of country interrelationships over time. For this purpose, Fig. B.11 shows the same directed weighted GFEVD spillover network obtained from the country aggregation of the GFEVD phase by phase.

In Tables 1 and 2, we report our results regarding the hubs and authorities algorithm performed on the GFEVD network. In particular, Table 1 shows countries ranked in decreasing order along with their "Hubs" value (in brackets) calculated on the directed network of country block GFEVDs divided into the four sub-samples under consideration. On the other hand, Table 2 reports countries ranked in decreasing order along with their "Authorities" values.

The premise of the hubs and authorities analysis is that there are two types of central nodes: authorities, that contain reliable information on the forecast error variance of the others, and hubs, that point to authoritative information on such forecast error variance. Results show that there is a noticeable variability in the hub-authority relationships across European countries as regards to dominance in terms of sentiment and real economy spillovers.

Interestingly, we find that Netherlands exhibits both an authoritative and hub behavior during the first two phases, while it then loses its relevance in the network in the aftermath of the Global Financial Crisis. At the same time, Germany's hub score increases, meaning it starts pointing to reliable sources of shock transmission,

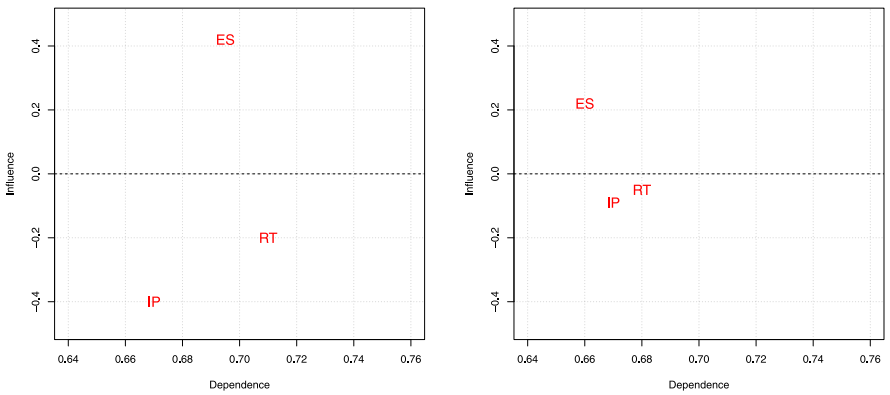

(a) Phase 1 (b) Phase 2

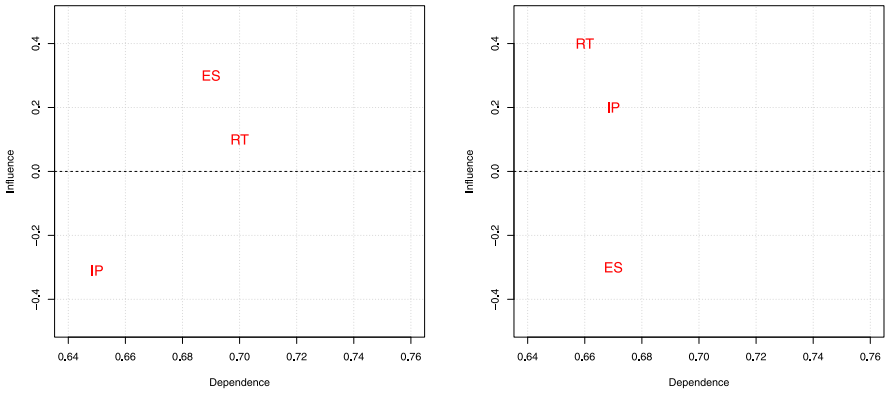

(c) Phase 3 (d) Phase 4

Fig. 3. Dependence-influence variable relationships. The figure shows a scatter plot obtained by generating a cartesian plane with the influence index on the x axis and the dependence index on the y axis. Both the indices are calculated from the country aggregation of the rolling GFEVDs. "IP" stands for Industrial Production, "RT" for Retail Trade and "ES" for Economic Sentiment.

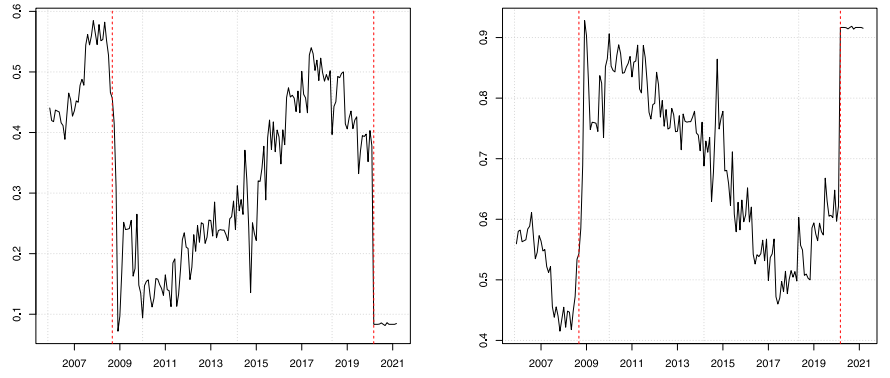

(a) Aggregate Heatwave (b) Spillover index

Fig. 4. Country Aggregate Heatwave and Spillover index. The figure shows the Aggregate Heatwave and Overall Spillover index based on the dynamic GFEVDs. Results are obtained by using a rolling window $w = 84$ and considering a $H = 40$ step ahead forecast horizon. The beginning of the Global Financial Crisis (September 2008) and the COVID-19 outbreak (February 2020) are marked in red. (For interpretation of the references to color in this figure legend, the reader is referred to the web version of this article.)

both during the tranquil period before COVID-19 and in the midst of the pandemic itself. In accord with the results on the dependence index, we additionally find that there is no predominant authority during the COVID-19 period, meaning that such large exogenous shock has affected the lead–lag relationships across countries, leveling out the authoritative behavior of dominant countries in the network.

5. Conclusions

We propose a methodology which takes root from the statistical and econometric literature concerning generalized forecast error variance decomposition of multivariate time series models. We build on a dynamic spillover network framework derived from a Global VAR

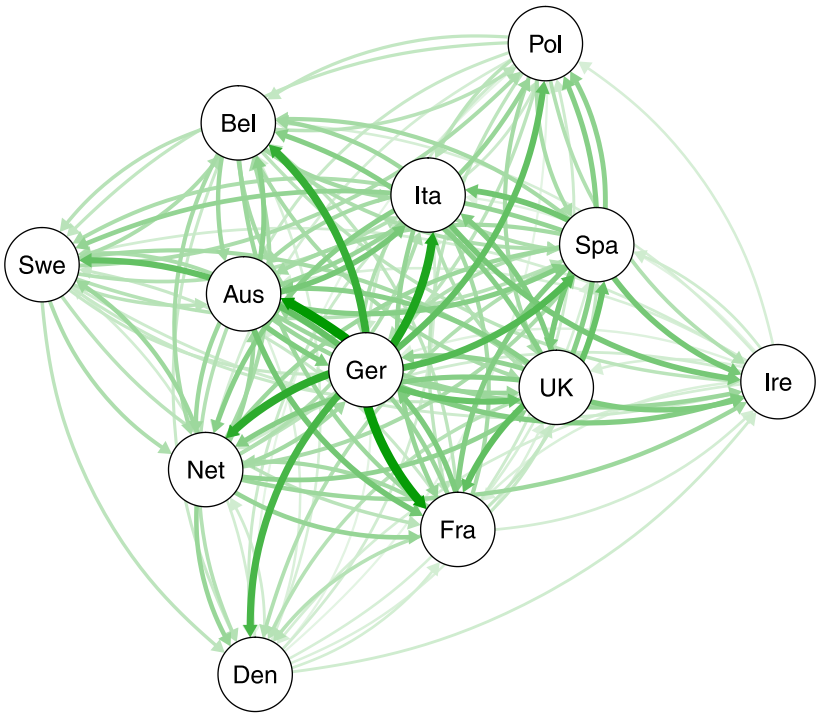

Fig. 5. Directed GFEVD country spillover network. The figure shows the directed weighted GFEVD spillover network obtained from the country aggregation of the whole sample GFEVD. Nodes represent countries, whereas links represent the magnitude of pairwise directed forecast error variance transmitted to others. Results refer to the whole sample period. Self-loops are omitted from the graphical representation.

Table 2
Country-level network authorities. The table reports countries ranked in decreasing order along with their normalized "Authorities" values (in brackets) calculated on the directed network of country block GFEVDs divided into the four sub-samples under consideration.

	1st	2nd	3rd	4th	5th
Phase 1	Net (10.380)	Bel (9.300)	Pol (9.064)	UK (8.993)	Den (8.245)
Phase 2	Net (9.793)	Spa (8.954)	Ger (8.685)	UK (8.578)	Swe (8.278)
Phase 3	Ger (9.504)	Spa (9.023)	Net (8.930)	Pol (8.893)	Ita (8.531)
Phase 4	Spa (8.341)	Ire (8.340)	Fra (8.340)	Net (8.338)	UK (8.337)

model, a suitable macroeconometric model to consider for simultaneous multi-level interdependencies. We then propose to exploit concepts from network theory to analyze the backbone structure, to perform community detection and to examine the hub-authority dynamics of longitudinal time series networks, both across countries and variables. We exemplify our method with an empirical application to study the network topology of spillover indices across a set of European countries, macroeconomic variables and sentiment data over the period 01/2000–11/2021.

We demonstrate the usefulness of our method to analyze the network structure of shock propagation in longitudinal time series and, in particular: (a) the shortest paths of contagion; (b) the clusters of shock transmission; (c) the role of nodes in the risk transmission channels. Our main results show how different crises exert starkly diverse impacts on real economy, economic sentiment and on the entire countries' macroeconomic network structure. In particular, while the impact of the Global Financial Crisis shows different consequences on the network interrelationships of macroeconomic variables if compared to those of the COVID-19 outbreak, the latter seems to be more persistent over time.

Despite the merit of our method in linking econometrics and network theory to produce advances in a cutting-edge research ground, there is room for methodological developments and empirical applications at the intersection of two fields – see for instance Celani and Pagnottoni (2023). While econometric models are often robust, yet not exploited from a network perspective, network models can constitute a precious contribution to the understanding of time series model outputs and, more generally, to the establishment of new cross-cutting disciplines. This is a promising avenue for future research not only in the context of real economy networks, but also on financial, social and any kind of networks.

CRediT authorship contribution statement

Alessandro Celani: Conceptualization, Data curation, Formal analysis, Investigation, Methodology, Software, Validation, Visualization, Writing – original draft, Writing – review & editing. **Paola Cerchiello:** Conceptualization, Funding acquisition, Investigation, Writing – original draft, Writing – review & editing, Formal analysis. **Paolo Pagnottoni:** Conceptualization, Formal analysis, Investigation, Methodology, Visualization, Writing – original draft, Writing – review & editing, Validation.

Acknowledgments

We thank the Editor, Guest Editors and two anonymous Referees for useful comments which have notably improved the paper. We also thank the organizers and participants of the "IV Conference on Financial Stability" for constructive feedback on an earlier version of the paper. This research has received funding from the European Union's Horizon 2020 research and innovation program "PERISCOPE: Pan European Response to the ImpactS of COVID-19 and future Pandemics

and Epidemics", under the grant agreement No. 101016233, H2020-SC1-PHE-CORONAVIRUS-2020-2-RTD. An earlier version of this paper circulated under the title "COVID-19, Macroeconomic Dynamics and Fear in Europe: a Network Global VAR Approach".

Appendix A. Methodological appendix

A.1. Global VAR forecast error variance decomposition

Given the nature of the variables underlying the Global VAR dynamical system, we follow Greenwood-Nimmo et al. (2021) who propose an aggregation scheme for the GFEVD in order to reduce its dimensionality with a direct interpretation on the countries (variables) FEVD. First, we re-normalize such that $\mathbb{C}_R^{(h)} = K$. After re-normalization, the (i, j) -th element of $\mathrm{C}_R^{(h)}$ represents the proportion of the total h -steps-ahead FEV of the system accounted for by the spillover effect from variable i to variable i. With this modification we are ensured that we may achieve a percentage interpretation even after aggregating groups of variables in the system.

Suppose we are interested in analyzing the spillover measures developed by Diebold and Yılmaz (2014) but focusing on the countries. It makes sense to aggregate the FEVD according to country blocks, where each ith element is obtained as an aggregation (sum) of the ith country block with its own variables. If, instead, the aim is to carry a variable analysis, the aggregation can be done considering the variable blocks.

Once we have collected $\mathbf{x}_t$ into b groups $\mathbb{C}_R^{(h)}$ can be equivalently expressed as:

$$\underset{(m\times m)}{\mathbb{C}_R^{(h)}} = \begin{bmatrix} \mathbf{B}_{1\leftarrow 1}^{(h)} & \mathbf{B}_{1\leftarrow 2}^{(h)} & \cdots & \mathbf{B}_{1\leftarrow b}^{(h)} \\ \mathbf{B}_{2\leftarrow 1}^{(h)} & \mathbf{B}_{2\leftarrow 2}^{(h)} & \cdots & \mathbf{B}_{2\leftarrow b}^{(h)} \\ \vdots & \vdots & \ddots & \vdots \\ \mathbf{B}_{b\leftarrow 1}^{(h)} & \mathbf{B}_{b\leftarrow 2}^{(h)} & \cdots & \mathbf{B}_{b\leftarrow b}^{(h)} \end{bmatrix}.$$

Let us stress that no information is lost in this process. Consider all the blocks lying on the main diagonal of that matrix (i.e. $\mathbf{B}_{k\leftarrow k}^{(h)}$); they contain all of the within-group FEV contributions. We can therefore define the within-group FEV contribution for the k th group as follows

$$\mathcal{W}_{k\leftarrow k}^{(h)} = \mathbf{e}'_{m_k} \mathbf{B}_{k\leftarrow k}^{(h)} \mathbf{e}_{m_k},$$

where $\mathbf{e}_{m_k}$ is the usual selection vector. Roughly speaking, the within-group FEV contribution for the k th group is equal to the sum of the elements of the block $\mathbf{B}_{k\leftarrow k'}^{(h)}$. Analogously, $\mathbf{B}_{k\leftarrow \ell}$ for $k \neq \ell$ relates to the transmission of information across groups. Hence we define the spillover from group ℓ to group k as $\mathcal{F}_{k\leftarrow \ell}^{(h)} = \mathbf{e}'_{m_k} \mathbf{B}_{k\leftarrow \ell}^{(h)} \mathbf{e}_{m_\ell}$ and the spillover to group k from group ℓ as $\mathcal{T}_{\ell\leftarrow k}^{(h)} = \mathbf{e}'_{m_\ell} \mathbf{B}_{\ell\leftarrow k}^{(h)} \mathbf{e}_{m_k}$. By collecting all these measures, we can define the h-step ahead block connectedness matrix of dimension $b \times b$ as

$$\underset{(b\times b)}{\mathbb{B}^{(h)}} = \begin{bmatrix} \mathcal{W}_{1\leftarrow 1}^{(h)} & \mathcal{F}_{1\leftarrow 2}^{(h)} & \cdots & \mathcal{F}_{1\leftarrow b}^{(h)} \\ \mathcal{F}_{2\leftarrow 1}^{(h)} & \mathcal{W}_{2\leftarrow 2}^{(h)} & \cdots & \mathcal{F}_{2\leftarrow b}^{(h)(h)} \\ \vdots & \vdots & \ddots & \vdots \\ \mathcal{F}_{b\leftarrow 1}^{(h)} & \mathcal{F}_{b\leftarrow 2}^{(h)} & \cdots & \mathcal{W}_{b\leftarrow b}^{(h)} \end{bmatrix}.$$

Note that the dimension of this grouped matrix is $b^2 < K^2$, which implies a significant improvement on the FEVD interpretation in large models ease the processing constraints encountered in large models. It is now straightforward to develop aggregate connectedness measures at the group level.

Appendix B. Empirical application

B.1. Data description and preliminary analysis

Among the economic variables, we analyze the Industrial Production index, a business cycle indicator which measures monthly changes in the price-adjusted output of industry. The second variable is the index of the volume of Retail Trade, a business indicator which measures the monthly changes of the deflated turnover of Retail Trade both at the level of the European Union (EU) and of the Eurozone. Both the economic indices are provided in their seasonally and calendar adjusted versions and normalized to 100 for the year 2015. As a measure of sentiment and expectations towards the future of economies, we select a third variable, i.e. the monthly Economic Sentiment index provided by the Directorate-General for Economic and Financial Affairs

Table B.3
Variables' descriptive statistics. The table reports summary descriptive statistics of the country variables over the whole sample period. The last column (p-val(JB)) reports the p-value of the Jarque–Bera normality test. All the statistics are computed on the log-level of variables.

Var.	Cou.	Mean	Median	Max	Min	Std	Skew	Kurt	p-val(JB)
	AUS	4.531	4.568	4.788	4.198	0.144	−0.379	2.204	0.002
	BEL	4.540	4.590	4.780	4.173	0.142	−0.544	2.146	0.000
	DEN	4.675	4.684	4.805	4.498	0.068	−0.177	1.939	0.002
	FRA	4.644	4.640	4.748	4.217	0.062	−1.579	11.189	0.000
	GER	4.522	4.562	4.685	4.261	0.101	−0.355	1.715	0.000
IND	IRE	4.229	4.141	4.864	3.657	0.266	0.504	2.303	0.000
	ITA	4.712	4.676	4.892	4.083	0.112	−0.715	5.696	0.000
	NET	4.609	4.616	4.729	4.503	0.042	−0.307	2.555	0.050
	POL	4.379	4.440	4.896	3.800	0.306	−0.334	1.951	0.000
	SPA	4.712	4.663	4.918	4.242	0.118	−0.023	2.420	0.186
	SWE	4.654	4.647	4.795	4.513	0.062	0.210	2.413	0.070
	UK	4.639	4.636	4.712	4.344	0.047	−1.377	9.240	0.000
	AUS	4.584	4.583	4.717	4.463	0.041	0.257	3.406	0.089
	BEL	4.560	4.585	4.735	4.440	0.062	−0.485	2.383	0.001
	DEN	4.631	4.625	4.809	4.524	0.058	0.194	2.534	0.156
	FRA	4.490	4.487	4.805	4.188	0.153	0.063	2.001	0.005
	GER	4.591	4.568	4.813	4.508	0.062	1.443	4.270	0.000
RET	IRE	4.565	4.511	4.905	4.209	0.124	0.565	2.323	0.000
	ITA	4.645	4.657	4.731	4.236	0.060	−1.779	11.875	0.000
	NET	4.644	4.638	4.772	4.558	0.046	0.410	2.535	0.009
	POL	4.456	4.490	4.904	4.020	0.245	−0.037	1.958	0.004
	SPA	4.719	4.715	4.907	4.328	0.105	−0.196	2.466	0.107
	SWE	4.430	4.469	4.777	4.022	0.208	−0.401	1.988	0.000
	UK	4.524	4.516	4.804	4.199	0.131	−0.290	3.015	0.162
	AUS	4.599	4.610	4.790	4.187	0.106	−1.189	5.431	0.000
	BEL	4.600	4.616	4.770	4.162	0.107	−1.461	6.084	0.000
	DEN	4.599	4.623	4.753	4.143	0.108	−1.655	7.125	0.000
	FRA	4.599	4.618	4.795	4.247	0.104	−0.960	4.541	0.000
	GER	4.600	4.633	4.757	4.275	0.105	−1.023	3.538	0.000
SENT	IRE	4.599	4.608	4.766	4.221	0.106	−1.184	4.908	0.000
	ITA	4.599	4.622	4.819	4.181	0.105	−0.944	3.972	0.000
	NET	4.599	4.617	4.765	4.230	0.105	−0.999	4.190	0.000
	POL	4.598	4.612	4.793	4.086	0.106	−1.149	6.549	0.000
	SPA	4.599	4.646	4.753	4.246	0.106	−1.166	3.837	0.000
	SWE	4.600	4.622	4.757	4.221	0.106	−1.188	4.575	0.000
	UK	4.598	4.628	4.750	4.177	0.109	−1.574	5.781	0.000

Table B.4
Augmented Dickey–Fuller tests. The table shows the value of the test statistics related to the Augmented Dickey–Fuller (ADF) tests performed on the first difference of our sample variables. The model specification for the null hypothesis of unit root is with constant but no time trend, and a lag selection based on the Akaike information criterion (AIC). The critical value according to our model specification is −2.89 considering a 5% significance level.

	Δ Ind. Production	ΔRet. Trade	ΔEconomic sentiment
AUSTRIA	−11.41	−11.13	−11.08
BELGIUM	−10.80	−10.53	−9.94
DENMARK	−10.43	−6.38	−11.46
FRANCE	−14.78	−11.62	−10.91
GERMANY	−13.66	−14.52	−8.971
IRELAND	−11.60	−11.02	−11.82
ITALY	−10.95	−11.90	−9.873
NETHERLANDS	−12.54	−15.83	−10.45
POLAND	−11.82	−12.05	−10.36
SPAIN	−14.04	−10.79	−12.69
SWEDEN	−13.08	−10.59	−10.47
UK	−12.15	−11.94	−11.08

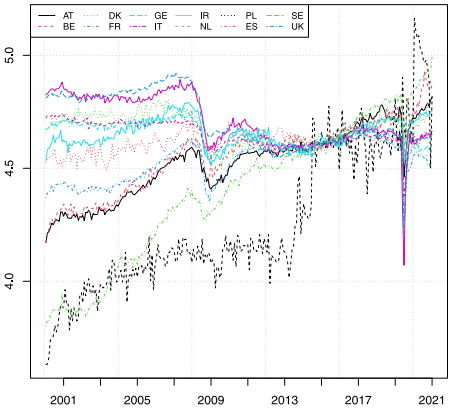

(a) Industrial Production

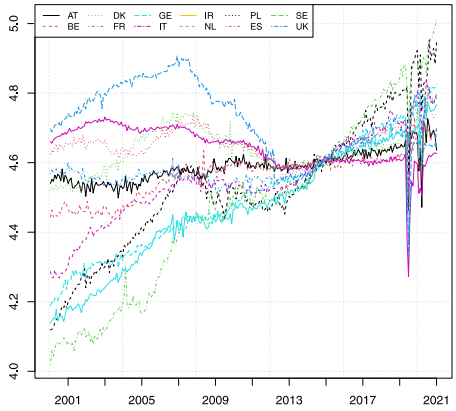

(b) Retail Trade

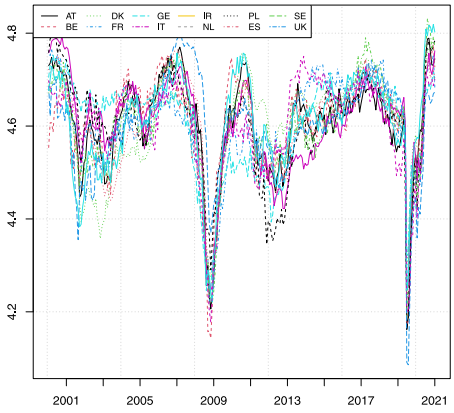

(c) Economic sentiment

Fig. B.6. Time series. The figure shows the dynamics of the time series of Industrial Production, Retail Trade and Economic Sentiment of the set of 12 analyzed European countries expressed in logarithmic terms over the whole sample period.

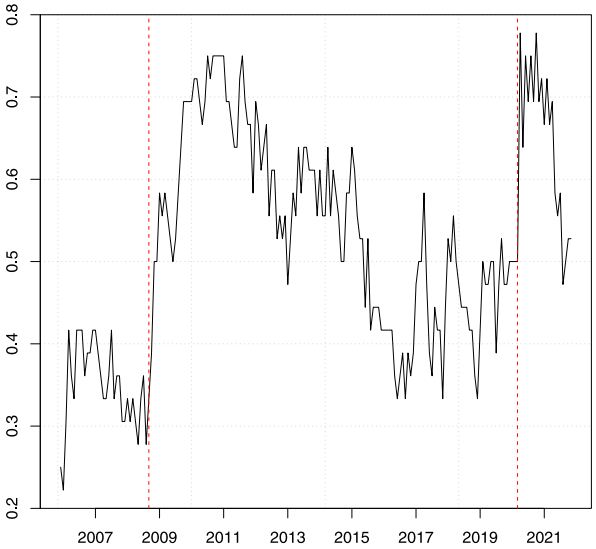

Fig. B.7. Fraction of significant cointegrating relationships. The figure shows the dynamics of total number of significant cointegrating relations in country models over the total number of possible cointegrating relationships (black line). The beginning of the Global Financial Crisis (September 2008) and of the COVID-19 outbreak (February 2020) are marked in red. Results refer to the Johansen Maximum Eigenvalue test for multiple cointegrating relationships considering a significance level of 10%.

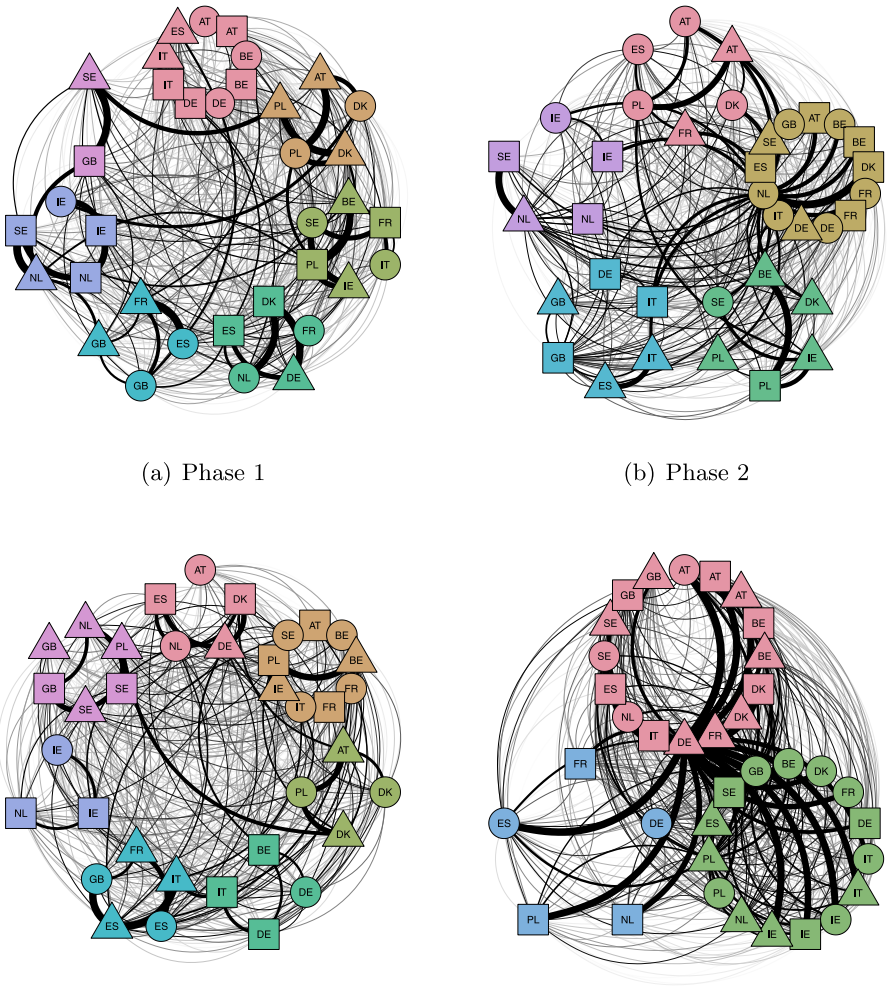

(a) Phase 1 (b) Phase 2

(c) Phase 3 (d) Phase 4

Fig. B.8. Sub-sample global forecast error variance clustering. The figure shows the clustered generalized forecast error variance decomposition (GFEVD) network structure of real economy and economic sentiment variables, where groups are classified according to the Louvain clustering algorithm. Squares: Industrial Production, triangles: Retail Trade, circles: Economic Sentiment.

Table B.5
F-statistics for testing the weak exogeneity of the country-specific foreign variables. CR is the number of cointegrating relationship found in the single country model.

Country	p_i	q_i	C. R.	Crit. Val.	IND	RET	SENT
AT	1	1	2	F(2,250)	0,780	5,224*	3,855
BE	3	3	2	F(2,236)	0,478	0,265	0,577
DK	1	1	0	F(0,252)			
FR	3	2	2	F(2,239)	1,275	4,122	0,108
GE	2	2	0	F(0,245)			
IR	1	1	0	F(0,252)			
IT	3	3	1	F(1,237)	2,502	2,486	3,166
NL	1	1	0	F(0,252)			
PL	1	1	0	F(0,252)			
SP	1	2	1	F(1,247)	0,527	0,671	0,241
SE	1	1	1	F(1,251)	4,442	7,490*	0,996
UK	1	1	1	F(1,251)	6,681*	0,002	0,229

* Denotes statistical significance at the 1% level.

(DG ECFIN). The indicator is calculated on the basis of a selection of questions from six different sectors and different topics:

- Consumer: financial situation, general economic situation, price trends, unemployment;
- Industry: production, employment expectations, stocks of finished products and selling price;
- Services: business climate, evolution of demand, evolution of employment and selling prices;
- Financial services: business situation, evolution of demand and employment;
- Retail Trade: business situation, stocks of goods, orders placed with suppliers and firm's employment;
- Construction: trend of activity, order books, employment expectations, price expectations and factors limiting building activity.

Each indicator is the core of the surveys which leads to the construction of sectorial monthly confidence indices, aimed at reflecting the overall perceptions and expectations at the individual sector level in a one-dimensional index. Economic Sentiment is then formulated by aggregating information from the six confidence indices, obtaining a comprehensive measure which is able to track the overall economic activity. All of the economic variables are publicly available and provided by EUROSTAT.[2]

As far as the weights matrix used to build the foreign variables of the country models, we use the annual data on bilateral trade flows, which are made publicly available by the International Monetary Fund

[2] Available at EUROSTAT: https://ec.europa.eu/eurostat/data/database.

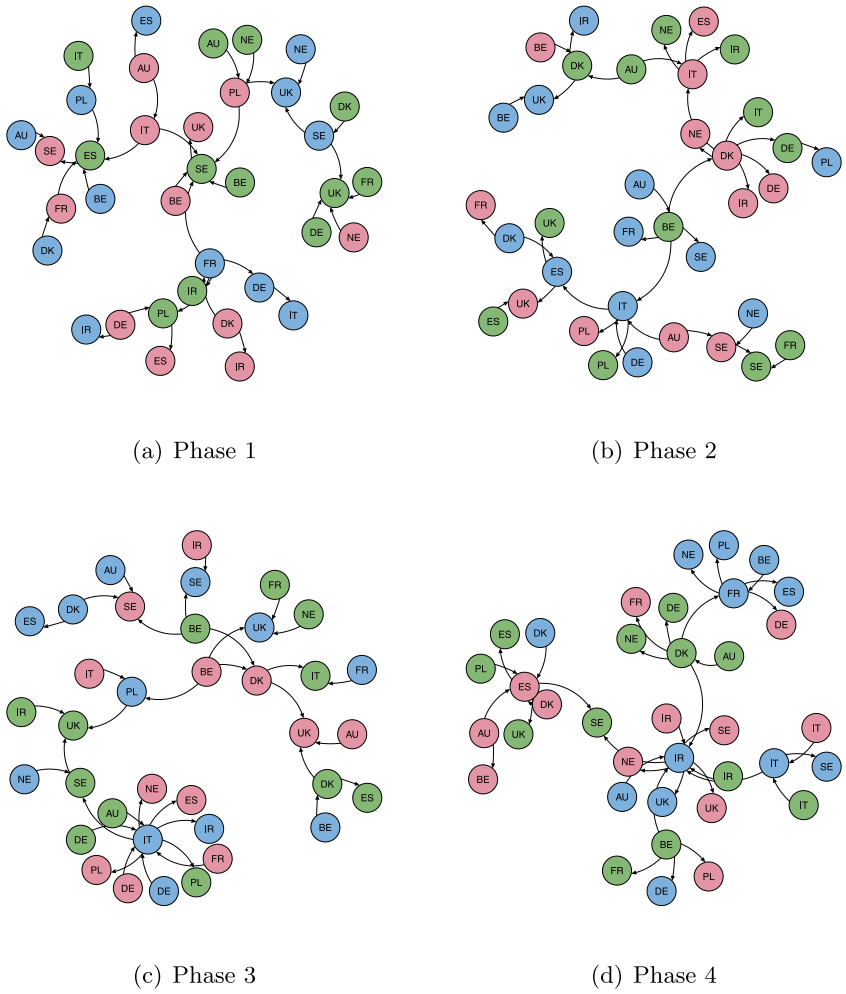

(a) Phase 1 (b) Phase 2

(c) Phase 3 (d) Phase 4

Fig. B.9. Sub-sample global forecast error variance Minimum Spanning Trees (MSTs). The figure shows the MST representation derived from the generalized forecast error variance decomposition (GFEVD) relative to the four periods of interest. Network nodes represent system variables, whereas edges represent the directional contribution of each variable to the forecast error variance decomposition of the others. Colors stand for Industrial Production (red), Retail Trade (green) and Economic Sentiment (blue). Self-loops are omitted. (For interpretation of the references to color in this figure legend, the reader is referred to the web version of this article.)

(IMF).[3] We therefore define $\omega_{ij} = \omega_{ji}$ as the sum of the import and export of country i with country j.

We report summary descriptive statistics of the country log-level variables over the whole sample period in Table B.3, along with the p-value of the Jarque–Bera normality test. Evidence shows both high cross-variable and cross-country variability, especially with regards to the real economic variables considered. In particular, both Industrial Production and Retail Trade show, for most of the countries, a relatively high variability, with peaks reached by the Polish Industrial Production (Std: 0.306) and Retail Trade (Std: 0.245). On the other hand, Economic Sentiment is fairly aligned across countries, which show both comparable values and variability. We can additionally conclude that the vast majority of the time series do not satisfy the normality test, meaning the joint null hypothesis of the skewness being zero and the excess kurtosis being zero is in most cases rejected by the Jarque–Bera test.

Table B.4 shows the Augmented Dickey–Fuller (ADF) test results performed on the first differences of our single country variables over the full sample period. We specify as a null hypothesis of unit root test a model with constant but no time trend, and a lag selection based on the Akaike information criterion (AIC). Evidence shows that, for all variables, the unit root hypothesis is rejected, hence, all of them are $I(1)$ in levels, meaning that stationarity is achieved by first differencing our set of economic and sentiment variables.

Fig. B.6 shows the dynamics of the time series of Industrial Production, Retail Trade and Economic Sentiment of the set of 12 analyzed European countries over the whole sample period. It evidently appears how different are the time series in their temporal dynamics. As for the Industrial Production and Retail Trade indicators, countries have particularly different values in the first half of the time series, while starting from 2016 values tend to converge. Moreover, we can spot a clear drop along all the time series in 2020 (COVID-19 pandemic) and another significant one in 2009–2010, with major evidence on the sentiment index.

B.2. Weak exogeneity test

A first estimation attempt consists of using OLS to estimate the single country VARX models. However, it is well known that The main assumption underlying the estimation of the individual country VARX models is the weak exogeneity of $\mathbf{x}_{it}^{*}$ with respect to the long run parameters of the conditional model. This assumption might be in practice violated.

For this reason, we firstly estimate the single country VARX models by means of OLS, and then verify the validity of this assumption through the weak exogeneity test outlined in ??. The results are reported in Table B.5.

[3] Available at IMF: https://data.imf.org/?sk=9D6028D4-F14A-464C-A2F2-59B2CD424B85&sId=1409151240976.

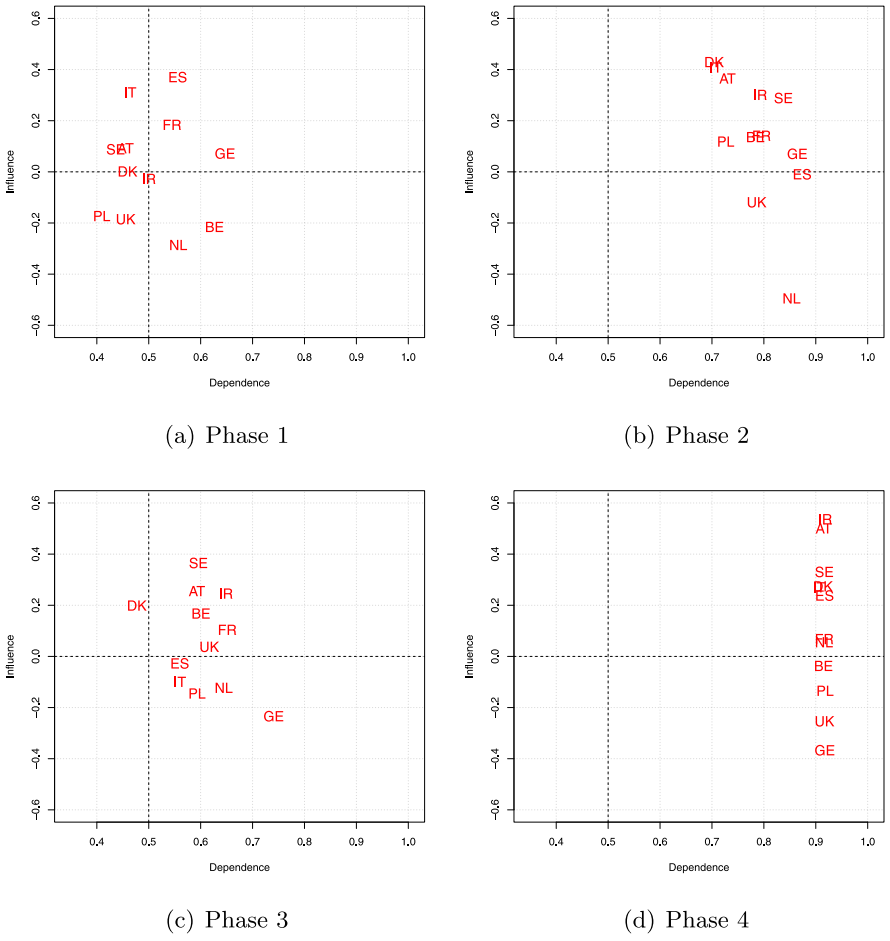

Fig. B.10. Dependence-influence country relationships. The figure shows a scatter plot obtained by generating a Cartesian plane with the influence index on the x axis and the dependence index on the y axis. Both the indices are calculated from the country aggregation of the rolling GFEVDs.

The weak exogeneity assumptions are rejected only in 3 cases out of 21. The first one pertains Industrial Production of UK, which is consistent with Dees et al. (2007), who found a rejection in the UK country model. The second and third ones are Retail Trade of Austria and Sweden. Given these premises and the suggestion of an anonymous Referee, we change our modeling strategy towards a more consistent estimation procedure outlined in the methodological section.

B.3. Global analysis

In order to measure the impacts of shocks on the real economy, the economic sentiment and their interrelationships across countries on a time-varying basis, we conduct a dynamic analysis. In other words, we set a rolling window w to estimate the Bayesian GVAR parameters and we obtain time varying estimates of the global forecast error variance decomposition connectedness measures. Our results are therefore obtained considering a Bayesian GVAR model based on twelve countries approximating VAR models estimated dynamically on a rolling window basis of six years and an H step ahead forecast horizon of 40 months.

As a preliminary analysis, we dynamically test for possible cointegrating relations among time series (in log-levels) through the Johansen Maximum Eigenvalue test. Fig. B.7 shows the proportion of significant cointegrating relationships with respect to the total number of possible cointegrating relationships present in the country models. Results clearly highlight that the number of cointegrated relationships tends to increase during crisis periods (see the Global Financial Crisis and the COVID-19 outbreak periods). This is equivalent to say that, in turbulent times, Industrial Production, Retail Trade and Economic Sentiment start to co-move more significantly. Interestingly, first evidence on the COVID-19 period supports the fact that the number of cointegrating relationships were immediately larger due the COVID-19 outbreak, if compared to those observed during the financial crisis of 2008. In spite of this, the former had an instantaneous impact on the cointegrating relationships of the system variables, meaning that the shock seems to dissipate relatively quicker over time, while the latter had more persistent effects on time series co-movements.

Fig. B.9 shows the MST representation of the predictive spillover networks relative to the four periods of interest. It clearly appears a temporal dynamics in the backbone structure of the network.

Evidence shows that the GFEVD network clusters are not constant and evolve dramatically over time — see Fig. B.8. We can see that the COVID-19 period shows the strongest links and the denser structure. Moreover, the two crisis periods are completely divergent: during the Global Financial Crisis the network becomes sparser and with few relevant links. During the COVID-19 period, instead, not only does the intensity of links increase, but also their numerosity.

B.4. Country analysis

Fig. B.10 shows dependence-influence country relationships. The scatter plot is obtained by generating a Cartesian plane with the influence index on the x axis and the dependence index on the y axis. Both the indices are calculated from the country aggregation of the GFEVDs. Similarly to what happens in Fig. 3, the first three periods are again comparable, despite some variability in the country specific positions in terms of dependence-influence. The real change occurs in phase 4, in which countries are basically equal in terms of dependence (around

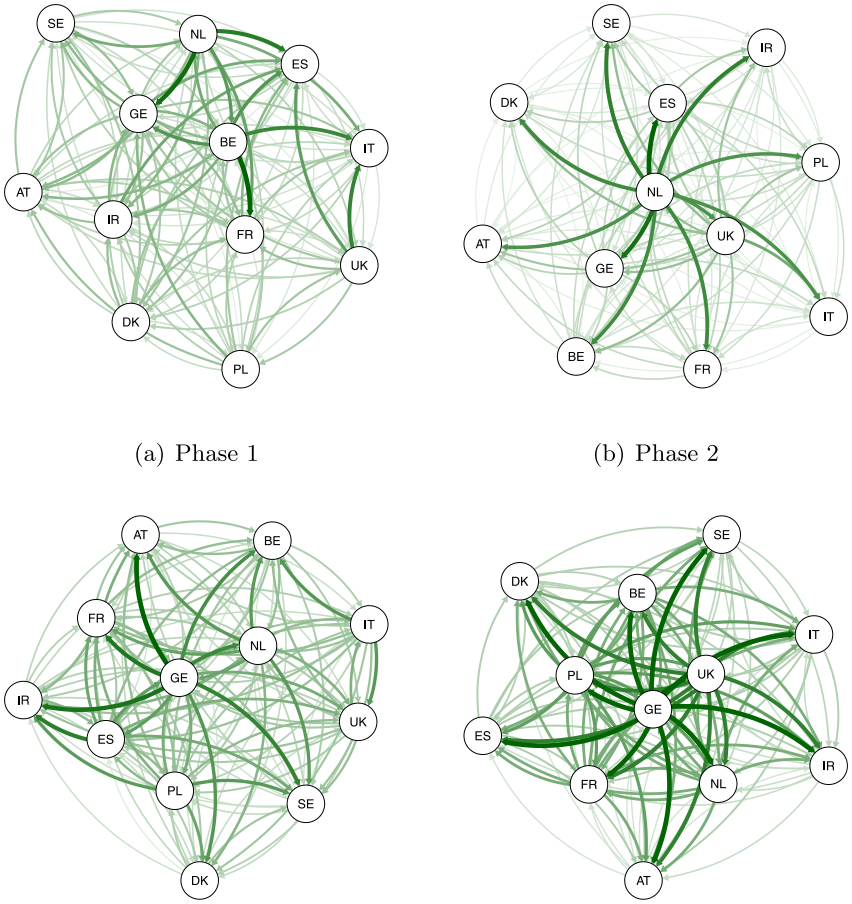

(a) Phase 1 (b) Phase 2

(c) Phase 3 (d) Phase 4

Fig. B.11. Directed GFEVD country spillover network. The figure shows the directed weighted GFEVD spillover network obtained from the country aggregation of the GFEVD phase by phase. Nodes represent countries, whereas links represent the magnitude of pairwise directed forecast error variance transmitted to others. Results are relative to the four sub-samples under analysis. Self-loops are omitted from the graphical representation.

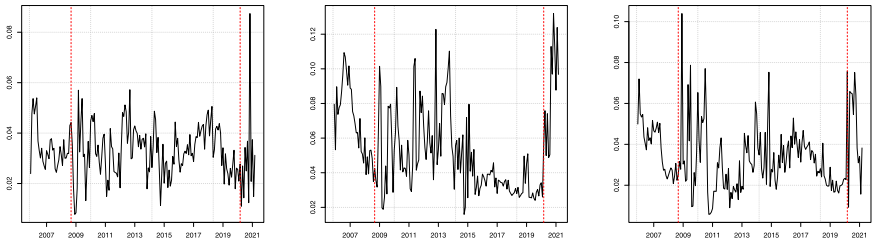

(a) Austria (b) Belgium (c) Denmark

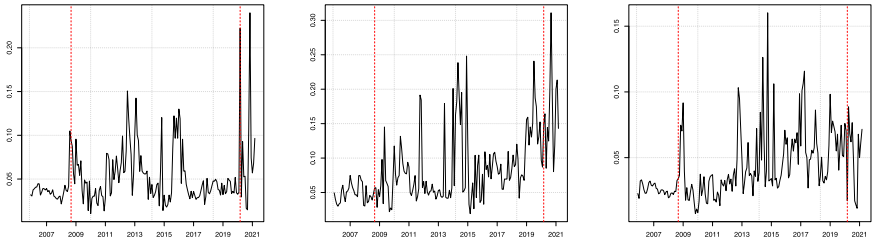

(d) France (e) Germany (f) Ireland

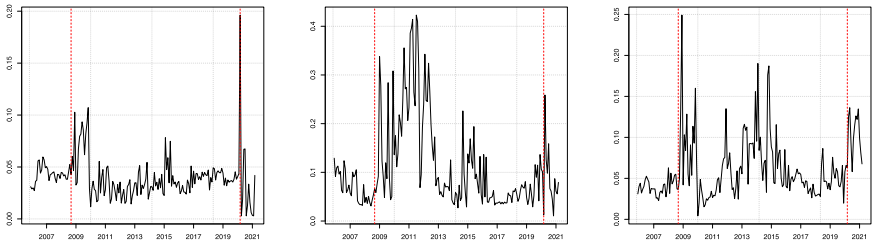

(g) Italy (h) Netherland (i) Poland

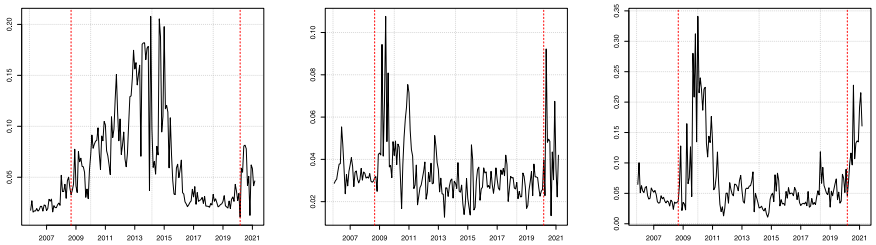

(j) Spain (k) Sweden (l) UK

Fig. B.12. Country FROM Spillover indices. The figure shows the time series dynamics of the From Spillover indices at a country-level. The beginning of the Global Financial Crisis (September 2008) and the COVID-19 outbreak (February 2020) are marked in red. (For interpretation of the references to color in this figure legend, the reader is referred to the web version of this article.)

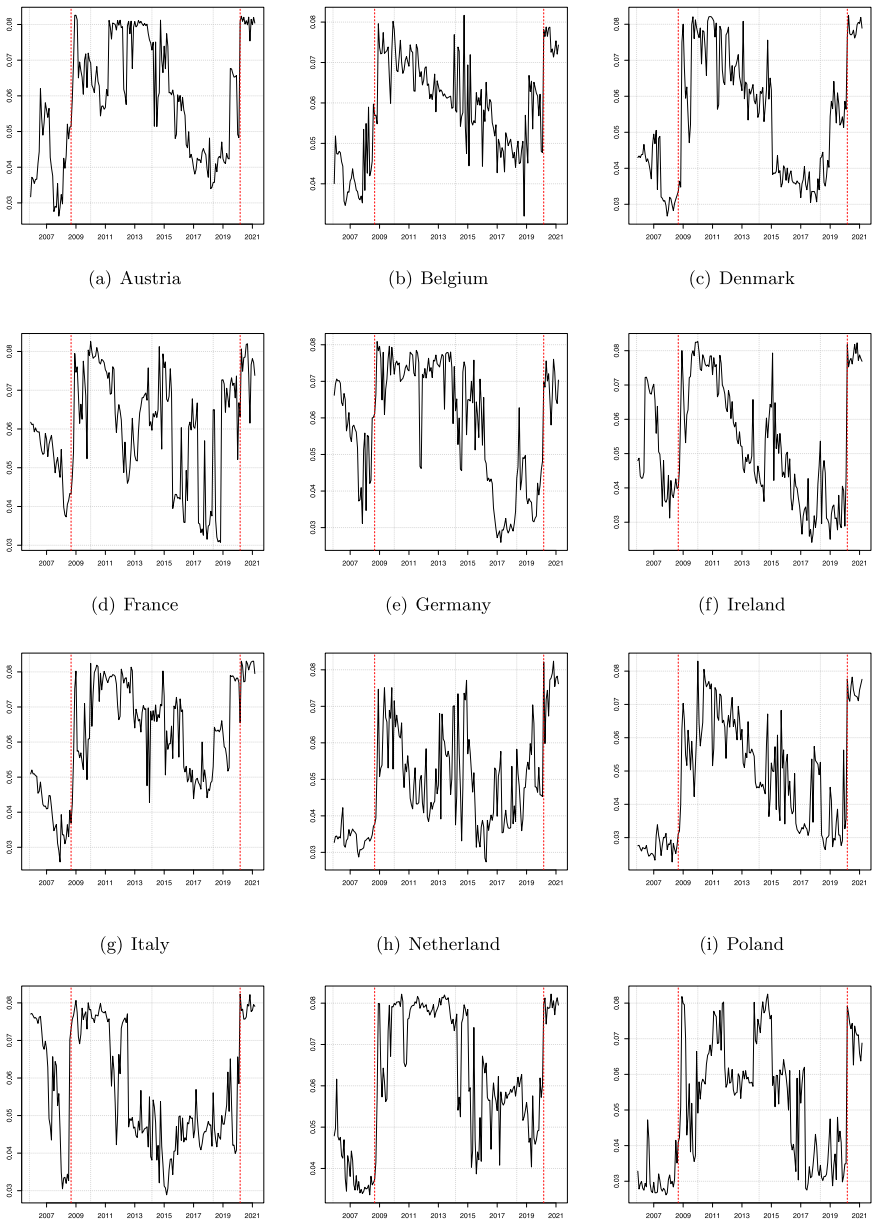

(a) Austria (b) Belgium (c) Denmark

(d) France (e) Germany (f) Ireland

(g) Italy (h) Netherland (i) Poland

(j) Spain (k) Sweden (l) UK

Fig. B.13. Country TO Spillover indices. The figure shows the time series dynamics of the To Spillover indices at a country-level. The beginning of the Global Financial Crisis (September 2008) and the COVID-19 outbreak (February 2020) are marked in red. (For interpretation of the references to color in this figure legend, the reader is referred to the web version of this article.)

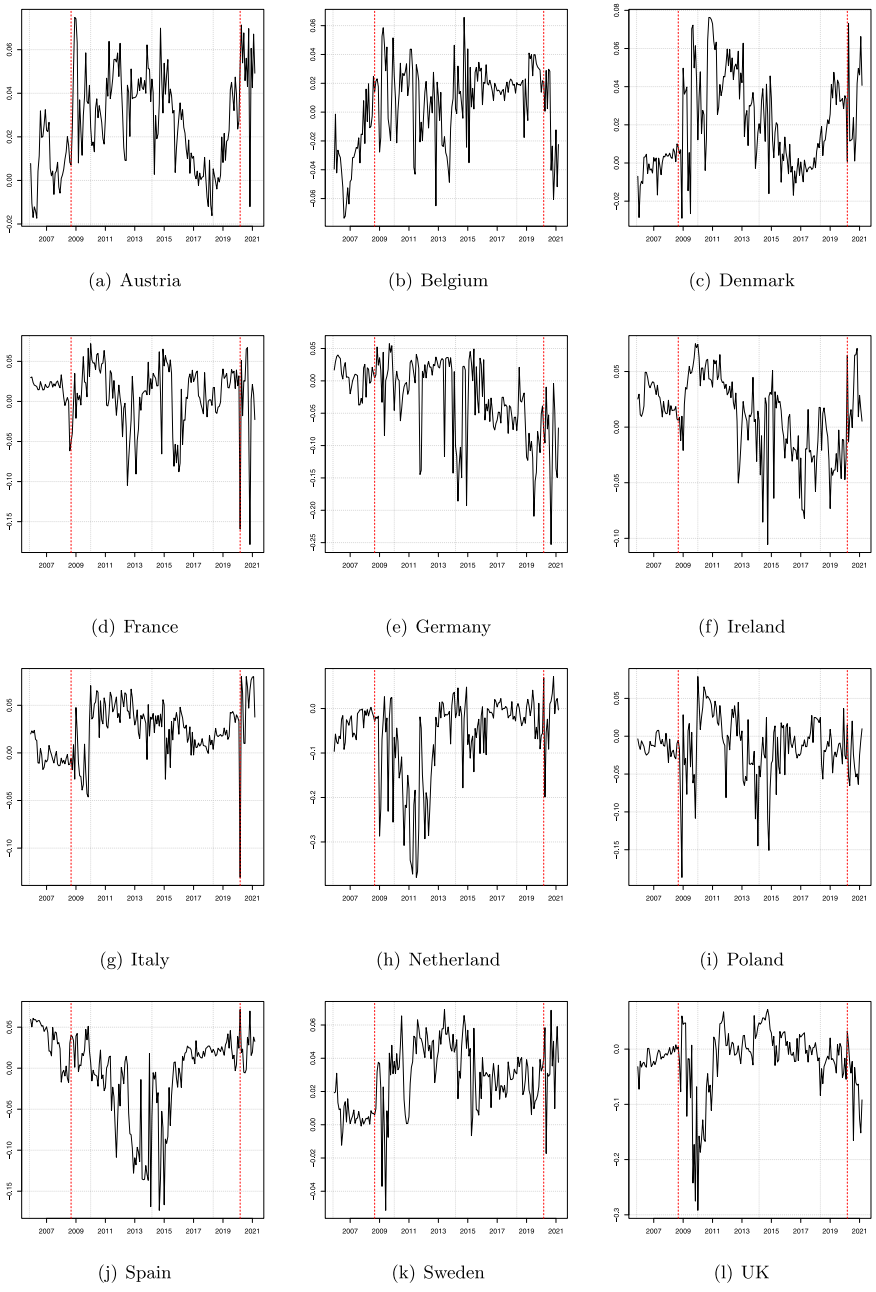

Fig. B.14. Country NET Spillover indices. The figure shows the time series dynamics of the Net Spillover indices at a country-level. The beginning of the Global Financial Crisis (September 2008) and the COVID-19 outbreak (February 2020) are marked in red. (For interpretation of the references to color in this figure legend, the reader is referred to the web version of this article.)

0.95), allegedly due to the effect of the exogenous shock exerted by the pandemic outbreak.

Fig. B.11 shows the directed weighted GFEVD spillover network obtained from the country aggregation of the GFEVD during the four phases under analysis. In accordance with the results of the hub and authority algorithms, we find that Netherlands is a central node in the network in terms of shock spreading power, especially during the Global Financial Crisis. Conversely, and still in line with the previous results, Germany appears to gain a pivotal role in the network in the aftermath of the Global Financial Crisis, which lasts even after the COVID-19 outbreak. We further report for completeness the estimated country FROM and TO spillover indices (see Figs. B.12 to B.14).

References

Ahelegbey, D.F., Billio, M., Casarin, R., 2016. Bayesian Graphical Models for Structural Vector Autoregressive Processes. J. Appl. Econometrics 31 (2), 357–386.

Ahelegbey, D.F., Cerchiello, P., Scaramozzino, R., 2022. Network based evidence of the financial impact of Covid-19 pandemic. Int. Rev. Financ. Anal. 81, 102101. http://dx.doi.org/10.1016/j.irfa.2022.102101, URL https://www.sciencedirect.com/science/article/pii/S1057521922000710.

Ahelegbey, D.F., Giudici, P., 2022. Netvix—A network volatility index of financial markets. Physica A 594, 127017.

Avdjiev, S., Giudici, P., Spelta, A., 2019. Measuring contagion risk in international banking. J. Financ. Stab. 42, 36–51.

Bardoscia, M., Battiston, S., Caccioli, F., Caldarelli, G., 2017. Pathways towards instability in financial networks. Nature Commun. 8 (1), 1–7.

Bartolucci, F., Pennoni, F., Mira, A., 2021. A multivariate statistical approach to predict COVID-19 count data with epidemiological interpretation and uncertainty

quantification. Stat. Med. 40 (24), 5351–5372. http://dx.doi.org/10.1002/sim.9129, arXiv:https://onlinelibrary.wiley.com/doi/pdf/10.1002/sim.9129, URL https://onlinelibrary.wiley.com/doi/abs/10.1002/sim.9129.

Battiston, S., Caldarelli, G., May, R.M., Roukny, T., Stiglitz, J.E., 2016. The price of complexity in financial networks. Proc. Natl. Acad. Sci. 113 (36), 10031–10036.

Battiston, S., Mandel, A., Monasterolo, I., Schütze, F., Visentin, G., 2017. A climate stress-test of the financial system. Nature Clim. Change 7 (4), 283–288.

Battiston, S., Monasterolo, I., Riahi, K., van Ruijven, B.J., 2021. Accounting for finance is key for climate mitigation pathways. Science 372 (6545), 918–920.

Battiston, S., et al., 2019. The importance of being forward-looking: managing financial stability in the face of climate risk. Financ. Stab. Rev. (23), 39–48.

Billio, M., Getmansky, M., Lo, A.W., Pelizzon, L., 2012. Econometric measures of connectedness and systemic risk in the finance and insurance sectors. J. Financ. Econ. 104 (3), 535–559.

Bitetto, A., Cerchiello, P., Mertzanis, C., 2021. A data-driven approach to measuring epidemiological susceptibility risk around the world.. Sci. Rep. 11.

Blondel, V.D., Guillaume, J.-L., Lambiotte, R., Lefebvre, E., 2008. Fast unfolding of communities in large networks. J. Stat. Mech.: Theory Exp. 2008 (10), P10008.

Bonacich, P., 2007. Some unique properties of eigenvector centrality. Soc. Netw. 29 (4), 555–564.

Brin, S., Page, L., 1998. The anatomy of a large-scale hypertextual web search engine. Comput. Netw. ISDN Syst. 30 (1–7), 107–117.

Burriel, P., Galesi, A., 2018. Uncovering the heterogeneous effects of ECB unconventional monetary policies across euro area countries. Eur. Econ. Rev. 101, 210–229. http://dx.doi.org/10.1016/j.euroecorev.2017.10.007, URL https://www.sciencedirect.com/science/article/pii/S0014292117301873.

Celani, A., Pagnottoni, P., 2023. Matrix autoregressive models: generalization and bayesian estimation. Studies in Nonlinear Dynamics & Econometrics.

Chudik, A., Pesaran, M.H., 2013. Econometric analysis of high dimensional VARs featuring a dominant unit. Econometric Rev. 32 (5–6), 592–649.

Chudik, A., Pesaran, M.H., 2016. Theory and practice of gvar modelling. J. Econ. Surv. 30 (1), 165–197. http://dx.doi.org/10.1111/joes.12095, arXiv:https://onlinelibrary.wiley.com/doi/pdf/10.1111/joes.12095, URL https://onlinelibrary.wiley.com/doi/abs/10.1111/joes.12095.

Cuaresma, J.C., Feldkircher, M., Huber, F., 2016. Forecasting with global vector autoregressive models: a Bayesian approach. J. Appl. Econometrics 31 (7), 1371–1391. http://dx.doi.org/10.1002/jae.2504, URL https://onlinelibrary.wiley.com/doi/abs/10.1002/jae.2504.

Dafermos, Y., Nikolaidi, M., Galanis, G., 2018. Climate change, financial stability and monetary policy. Ecol. Econom. 152, 219–234.

Dees, S., Mauro, F.d., Pesaran, M.H., Smith, L.V., 2007. Exploring the international linkages of the euro area: a global VAR analysis. J. Appl. Econ. 22 (1), 1–38.

Delis, M.D., Savva, C.S., Theodossiou, P., 2021. The impact of the coronavirus crisis on the market price of risk. J. Financ. Stab. 53, 100840.

Diebold, F.X., Yilmaz, K., 2009. Measuring financial asset return and volatility spillovers, with application to global equity markets. Econ. J. 119 (534), 158–171.

Diebold, F.X., Yilmaz, K., 2012. Better to give than to receive: Predictive directional measurement of volatility spillovers. Int. J. Forecast. 28 (1), 57–66.

Diebold, F.X., Yılmaz, K., 2014. On the network topology of variance decompositions: Measuring the connectedness of financial firms. J. Econometrics 182 (1), 119–134.

Diebold, F.X., Yılmaz, K., 2015. Financial and Macroeconomic Connectedness: A Network Approach To Measurement and Monitoring. Oxford University Press, USA.

Elhorst, J.P., Gross, M., Tereanu, E., 2018. Spillovers in space and time: where spatial econometrics and global VAR models meet.

Greenwood-Nimmo, M., Nguyen, V.H., Shin, Y., 2021. Measuring the connectedness of the global economy. Int. J. Forecast. 37 (2), 899–919.

Gross, M., Kok, C., 2013. Measuring contagion potential among sovereigns and banks using a mixed-cross-section GVAR.

Harris, J., Hirst, J.L., Mossinghoff, M., 2008. Combinatorics and Graph Theory. Springer New York, http://dx.doi.org/10.1007/978-0-387-79711-3.

Iwanicz-Drozdowska, M., Rogowicz, K., Kurowski, Ł., Smaga, P., 2021. Two decades of contagion effect on stock markets: Which events are more contagious? J. Financ. Stab. 55, 100907.

Katz, L., 1953. A new status index derived from sociometric analysis. Psychometrika 18 (1), 39–43.

Konstantakis, K.N., Michaelides, P.G., Tsionas, E.G., Minou, C., 2015. System estimation of GVAR with two dominants and network theory: Evidence for BRICs. Econ. Model. 51, 604–616.

Kose, M.A., Otrok, C., Whiteman, C.H., 2003. International business cycles: World, region, and country-specific factors. Am. Econ. Rev. 93 (4), 1216–1239.

Kose, M.A., Otrok, C., Whiteman, C.H., 2008. Understanding the evolution of world business cycles. J. Int. Econ. 75 (1), 110–130.

Litterman, R.B., 1986. Forecasting with Bayesian vector autoregressions: Five years of experience. J. Bus. Econom. Statist. 4 (1), 25–38, URL http://www.jstor.org/stable/1391384.

Liu, Y., Qiu, B., Wang, T., 2021. Debt rollover risk, credit default swap spread and stock returns: Evidence from the COVID-19 crisis. J. Financ. Stab. 53, 100855.

Micciché, S., Bonanno, G., Lillo, F., Mantegna, R.N., 2003. Degree stability of a minimum spanning tree of price return and volatility. Physica A 324 (1–2), 66–73.

Mishkin, F.S., 2011. Over the cliff: From the subprime to the global financial crisis. J. Econ. Perspect. 25 (1), 49–70.

Monasterolo, I., Battiston, S., Janetos, A.C., Zheng, Z., 2017. Vulnerable yet relevant: the two dimensions of climate-related financial disclosure. Clim. Change 145 (3), 495–507.

Musciotto, F., Marotta, L., Micciché, S., Mantegna, R.N., 2018. Bootstrap validation of links of a minimum spanning tree. Physica A 512, 1032–1043.

Pagnottoni, P., 2023. Superhighways and roads of multivariate time series shock transmission: application to cryptocurrency, carbon emission and energy prices. Physica A: Statistical Mechanics and its Applications 615, 128581.

Pagnottoni, P., Spelta, A., 2023. The motifs of risk transmission in multivariate time series: application to commodity prices. Socio-Economic Planning Sciences 87, 101459.

Pagnottoni, P., Spelta, A., Flori, A., Pammolli, F., 2022. Climate change and financial stability: Natural disaster impacts on global stock markets. Physica A 599, 127514.

Pagnottoni, P., Spelta, A., Pecora, N., Flori, A., Pammolli, F., 2021. Financial earthquakes: SARS-CoV-2 news shock propagation in stock and sovereign bond markets. Physica A 582, 126240.

Pesaran, M.H., Schuermann, T., Weiner, S.M., 2004. Modeling regional interdependencies using a global error-correcting macroeconometric model. J. Bus. Econom. Statist. 22 (2), 129–162. http://dx.doi.org/10.1198/073500104000000019, arXiv:https://doi.org/10.1198/073500104000000019.

Pesaran, M.H., Yang, C.F., 2020. Econometric analysis of production networks with dominant units. J. Econometrics 219 (2), 507–541.

Roncoroni, A., Battiston, S., Escobar-Farfán, L.O., Martinez-Jaramillo, S., 2021. Climate risk and financial stability in the network of banks and investment funds. J. Financ. Stab. 54, 100870.

Roukny, T., Battiston, S., Stiglitz, J.E., 2018. Interconnectedness as a source of uncertainty in systemic risk. J. Financ. Stab. 35, 93–106.

Sims, C.A., Zha, T., 1998. Bayesian methods for dynamic multivariate models. Internat. Econom. Rev. 39 (4), 949–968, URL http://www.jstor.org/stable/2527347.

Spelta, A., Pagnottoni, P., 2021. Mobility-based real-time economic monitoring amid the COVID-19 pandemic. Sci. Rep. 11 (1), 1–15.

Stolbova, V., Monasterolo, I., Battiston, S., 2018. A financial macro-network approach to climate policy evaluation. Ecol. Econom. 149, 239–253.